INVESTIGATION OF TRIBOLOGICAL PROPERTIES OF MICRO/NANO SIZED WC-CO HARDMETALS PREPARED BY SPARK PLASMA SINTERING PROCESS AT ELEVATED TEMPERATURES

BY

SALEH ABDULLAH AL WOHAIBI

A Thesis Presented to the

DEANSHIP OF GRADUATE STUDIES

KING FAHD UNIVERSITY OF PETROLEUM & MINERALS

DHAHRAN, SAUDI ARABIA

In Partial Fulfillment of the
Requirements for the Degree of

MASTER OF SCIENCE

In

MECHANICAL ENGINEERING

MAY - 2017

KING FAHD UNIVERSITY OF PETROLEUM & MINERALS

DHAHRAN, SAUDI ARABIA

DEANSHIP OF GRADUATE STUDIES

This thesis, written by **Saleh Abdullah Al-Wohaibi** under the direction of his thesis advisor and approved by his thesis committee, has been presented to and accepted by the Dean of Graduate Studies, in partial fulfillment of the requirements for the degree of MASTER OF SCIENCE in **Mechanical Engineering**

Thesis Committee

Thesis Advisor
Dr. Mohammad Abdul Samad

Member
Prof. Taher Laoui

Member
Dr. Abbas Hakeem

Department Chairman

Dr. Zuhair Mattoug Gasem

Dean of Graduate Studies

Prof. Salam Adel Zummo

17/12/17

Date

This research is dedicated with deepest love and gratitude to my source of hope; my family

……

My father Abdullah, my mother Mizna, my wife Fatimah and my lovely kids.

……

Their undying love, trust and encouragement continues to surround and support me in my journey as a son and as a father.

ACKNOWLEDGMENT

Firstly, I offer my thankfulness to my advisor, Dr. Mohammed Abdulsamad, who has helped me out, in technical, ethical and supported me throughout my

research, particularly his patience and guidance as allowing me to communicate at any time in a friendly manner.

It was an honor for me to be working under positive supervision of Prof. Taher Laoui. I appreciate his supervision and advices from the early stages of this research as well as giving me extraordinary experiences throughout the work.

I would like to thank also Dr. Abbas Hakeem for the most of what he attributes. He provided me steady encouragement and support in various ways personally or through the center of excellence in nanotechnology (CENT). His scientific comments and ideas have been always rich regarding this thesis work. I found him ready to help and discuss, when and ever I need.

I would like to thank the chairman of the mechanical engineering department, Dr. Zuhair Gasem, for the advices he offered. Also, I like to acknowledge all the department's staff who always help me whenever I need as a student or as a scientist.

My deep thanks to King Fahd University of petroleum and minerals (KFUPM), and in particular to Mechanical Engineering department for giving me an opportunity to step-up in my educational career. I enjoyed the entire supportive research oriented environment.

I cannot forget my family support and patience. My parents, my wife, my kids, brother and sisters, I truly admire their patience; I truly appreciate their motivation, their prayers and their encouragement in completing my thesis research.

CONTENTS

LIST OF TABLES

LIST OF FIGURES

LIST OF ABBREVIATIONS

SE	Secondary electron		
EDS	Energy dispersive spectroscopy		
WC	Tungsten carbide	XRD	X-ray diffraction

Co	Cobalt	Vs.	Versus
Al_2O_3	Aluminum oxide	HV	Vickers hardness
N	Neoteny	M	Meter
Al	Aluminum	S	Second
O	Oxygen	G	Grams
Ar	Argon	Hr	Hour
TaC	Tantalum Carbide	Min	Minute
SPS	Spark plasma sintering	MPa	Mega Pascal
HIP	Hot isostatic pressing	GPa	Giga Pascal
HP	Hot pressing	wt. %	Weight percentage
TiC	Titanium Carbide	Mm	Millie meter
UK	United Kingdom	Nm	Nano meter
USA	United States of America	Mm	Micro meter
SEM	Scanning electron microscope	2D	Two dimensions
BSE	Backscattered electron	3D	Three dimensions

ABSTRACT

Full Name : SALEH ABDULLAH AL WOHAIBI

Thesis Title : INVESTIGATION OF TRIBOLOGICAL PROPERTIES OF MICRO/NANO SIZED WC-CO HARDMETALS PREPARED BY SPARK PLASMA SINTERING PROCESS AT ELEVATED TEMPERATURES

Major Field : MECHANICAL ENGINEERING

Date of Degree : MAY-2017

Tungsten Carbide-Cobalt (WC-Co) cemented carbides are probably the first class of materials used by the hardmetals industry. They have remarkable mechanical properties such as high hardness, excellent high temperature strength, high elastic modulus, good wear resistance, corrosion resistance and excellent chemical stability at high temperature. These cemented carbides have been extensively used for cutting tool tip applications which demands high wear resistance, as the tool tip experiences high temperatures between the tool and chip during machining processes. Therefore, it is crucial to gain an understanding of the wear behavior of these carbides at room and at elevated temperatures.

Hence, this study aims to investigate the tribological performance of hardmetal composites reinforced with nano and micron sized tungsten carbide (WC) respectively, binded by 9 wt.% of cobalt (Co) at room and elevated temperatures. The composites were fabricated using a two-step procedure of mixing followed by spark plasma sintering (SPS). Ball on disc wear tests were conducted at three different normal loads (15N, 30N and 45N) and at three different linear speeds (0.1 m/s, 0.2 m/s and 0.4 m/s) under dry conditions and at three different temperatures (Room Temperature, 300°C and 600°C). Scanning Electron Microscopy (SEM), Optical Profilometry and Energy Dispersive X-ray (EDX) spectroscopy were used to characterize the surface morphology and the wear track area. At room temperature, it was observed that the nano sized WC composites showed better wear resistance as compared to the micron sized WC composites. However, the performance in terms of wear resistance of the nano sized samples decreased significantly as compared to the micron sized samples with an increase in temperature. This reduction in performance is attributed to the higher surface area of the nano sized WC particles which are exposed to rapid oxidation at elevated temperatures resulting in poor wear resistance. It is observed

that the wear rate at 600°C for the micron sized WC composites was 75% lower as compared to the wear rate of nano sized WC. Oxidative wear was observed to be the predominant wear mechanism for both sizes of WC samples at elevated temperatures.

ARABIC ABSTRACT

ملخص الرسالة

الاسم الكامل: صالح بن عبدالله الوهيبي

عنوان الرسالة: بحث الخصائص التريبولوجية في درجات الحرارة العالية للمركبات الميكروية والنانوية لكبريتيد التنجستن الكوبالتي المحضرة بالبلازما

التخصص: الهندسة الميكانيكية

تاريخ الدرجة العلمية: مايو – 2017م

كبريتيد التنجستن الكوبالتي (WC-Co) هو على الأرجح من أفضل أنواع مواد المصانع الصلبة بسبب خصائصها الميكانيكية المميزة كدرجة الصلابة و درجة تحملها لدرجات الحرارة العالية ولمعامل مرونتها العالي و لمقاومتها الجيدة للتآكل وتحملها للصدأ وثباتها الكيميائي الممتاز في درجات الحرارة العالية وتستخدم بكثرة في تطبيقات أدوات القطع التي تحتاج مقاومة عالية للتآكل لأن أدوات القطع تتعرض لدرجات حرارة عالية بين الأداة وبين البرادة المقطوعة أثناء عمليات الآلات و بالتالي من الاهمية فهم تآكل هذا المركب في درجة حرارة الغرفة و درجات الحرارة العالية.

تهدف الدراسة لتقديم بحث عن الخصائص التريبولوجية للمركبات النانوية و المايكروية من (WC) مع إضافة نسبة (9% Co) على مختلف درجات الحرارة و تم طحن كبريتيد التنجستن النانوي باستخدام جهاز الطحن الكروي عالي الطاقة ثم ضغطها و تصنيعها باستخدام البلازما (SPS) وتم اختبار التآكل باستخدام طريقة الكرة و القرص على ثلاثة أوزان (15N, 30N,45N) و على ثلاثة سرعات (0.1 m/s, 0.2 m/s,0.3m/s) بحالة جافة و على ثلاث درجات حرارة مختلفة (RT,300°C,600°C) و تم استخدام المسح الضوئي المجهري الالكتروني (SEM) وجهاز الرسم البصري وجهاز الأشعة السينية لتوصيف السطوح و مساحات التأكل .

لوحظ أن المركب النانوي يعطي ممانعة تآكلية أفضل بالمقارنة مع المركب المايكروي في درجة حرارة الغرفة بسبب أن المركبات النانوية لديها مساحة سطح أكبر يساعد الاحتكاك وتوزيع الأوزان ، بينما عند زيادة حرارة الاختبار يقل أداء المركب النانوي بشدة بسبب تعرض مساحة السطح للصدأ بشكل أكبر، وكذلك لوحظ أن التآكل بسبب الصدأ هو العامل الأكبر لكلا المركبين في درجات الحرارة العالية و تم عرض معدل التآكل للمركب المايكروي في درجة حرارة (600°C) أقل بنسبة 75 % من المركب النانوي

CHAPTER 1

1. INTRODUCTION

Tungsten Carbide-Cobalt (WC-Co) cemented carbides, also called as hardmetals are a group of sintered materials which are formed when hard transition metal carbide of the B subgroups IV-VI is merged with a tough metal binder of the B subgroup VIII. Cemented carbides are composite materials that have exceptional wear resistance and hardness, consisting of brittle refractory carbides of the transition metals (e.g. WC, TaC, and TiC) which are implanted in a metallic matrix. The success of this ceramic-metal composite resides in the combination of the wear resistance and hardness of ceramic particles with the toughness of the metallic phase.

Hardmetals have remarkable mechanical properties such as high hardness, excellent high temperature strength, high elastic modulus, good wear and corrosion resistance, chemical and thermal stability at high temperature. Therefore, they have a variety of applications ranging from bearings and mechanical face seals and press molds, cutting dies and material deforming tools, rock drilling, mining bits, sand blasting nozzles, and more importantly as cutting tools. Besides high hardness and wear resistance, a high thermal resistance makes WC-Co cemented carbides tools most suitable for dry cutting and high-speed machining.

Nowadays, there is a growing need for applying these materials to high fatigue loading tools and components. However, the main use of these materials to be used for cutting tool applications is wear resistance at room temperature and at extreme temperatures. So, to get those operative features of that hardmetal, all dynamics must be considered. Cemented carbides are composite materials that have remarkable wear resistance and hardness, consisting of brittle refractory

carbides of the transition metals (e.g. WC, TaC, and TiC [1]) which are implanted in a metallic matrix [2]. The success of this ceramic-metal composite resides in the combination of the wear resistance and hardness of ceramic particles with the toughness of the metallic phase. WC-Co hardmetals derive their strength and wear resistance from the presence of 85-95% fine WC particles whereas cobalt contributes to the toughness and ductility of the alloy [3]. Since the appearance of earliest WC–Co cemented carbides in 1923, cobalt has been the leading metal used as a binder in these metal-ceramic composite materials [3] because of its outstanding adhesion properties and carbide wetting [4]. As leader materials, cemented carbides are used in several engineering and tooling applications, such as metal cutting [5], face sealings [6], wear parts [7], structural mechanisms [8], mining bits [9], rock drilling [10] and bearings [11]. There is a growing demand for applying these materials to high fatigue loading tools and components. However, the major requirements for these materials to be used for cutting tool applications is wear resistance at room and at elevated temperatures. The high temperature strength and mechanical properties such as wear resistance of cemented carbides depends on various factors such as the volumetric content and chemical composition of the binder [12], average sizes of carbide phase grains and cobalt interlayers, value and mode of the application of mechanical load, temperature, deformation rate, and environment [13]. To attain the required operational characteristics of the structural hardmetal, all the above factors should be accurately accounted [14].

1.1Objectives

The aim of the present work is to develop a cemented carbide composed of tungsten carbide (WC) and 9 wt% cobalt (Co) binder for cutting tool applications, and evaluate its tribological performance at different parameters. The objectives of the present work are defined as follows:

- To synthesize dense WC-9wt% Co using two different particle sizes of WC (micro & nano) by Spark Plasma Sintering technique.
- To characterize the microstructure of the synthesized cemented carbides
- To study the tribological performance of the synthesized cemented carbides at different wear parameters including load and speed.
- To study the tribological performance of the synthesized cemented carbides at different temperatures including room temperature, 300 C, and 600 C.

1.2 Phases

To achieve the above objectives, the project was divided into different phases which are explained below:

PHASE 1: Development and characterization of the micron and nano sized WC-9wt%Co composites using spark plasma sintering technique

- **Task 1**: Optimize the milling and mixing parameters for the various powders
- **Task 2**: Characterize the powders in terms of particle sizes and morphology
- **Task 3**: Optimize the spark plasma sintering parameters such as sintering time, temperature and pressure. to obtain good samples
- **Task 4**: Characterize the samples in terms of micro structure, porosity and density

PHASE II: Tribological characterization of the prepared composite samples at room temperature

- **Task 1**: Surface preparation
- **Task 2**: Conducting wear tests to characterize the samples in terms of specific wear rates and coefficient of friction
- **Task 3**: Evaluate the effect of load

- **Task 4**: Evaluate the effect of speed
- **Task 5**: Conducting scanning electron microscopy to understand the underlying wear mechanisms.

PHASE III: Tribological characterization of the prepared samples at elevated temperatures

- **Task 1**: Designing and manufacturing of a proper fixture for holding samples in the tribometer
- **Task 2**: Running wear tests at elevated temperatures of 300°C and 600°C
- **Task 3**: Conducting scanning electron microscopy to understand the underlying wear mechanisms.

CHAPTER 2

2. LITERATURE REVIEW

2.1 The effect of different parameters on the tribological properties of hardmetals

2.1.1 Effect of particle sizes of WC and Co

The used optimum compacting conditions for the ultra-fine or the nano sized powders are sure different than the micron size powders. This easily can be understood because of the higher total surface area of nano sized powders [15]. Based on theoretical developments on the stability of dislocations in nanoparticles, the size range of the existence of WC nanoparticles and nanostructured WC–Co hard alloys has been defined, which is 5–40 nm [16]. Existing technologies - solid and liquid phase sintering, intensive heating and the use of high pressures - do not allow WC–Co pore free nanostructured hard alloys with particles of size 5–40 nm to be produced and Figure 1 shows the classification of WC-Co by sizes [16]. M. Gee [9] highlighted the observations of wear mechanism by using several abrasion, erosion and erosion-corrosion tests and studied the effect of WC grain size on abrasion volume loss, finding that decreasing of grain size and binder phase decreases abrasion volume loss. Also, C. Allen [17] indicated that wear rate increases with the increase of particle size in three body abrasion and particle erosion tests and concluded that with the variation in grain size from coarse to ultrafine the material removal mechanism shifts from extensive localized fragmentation of WC grains to ductile deformation and bulk removal of material which in turn made a prominent shift in the wear rate and resistance.

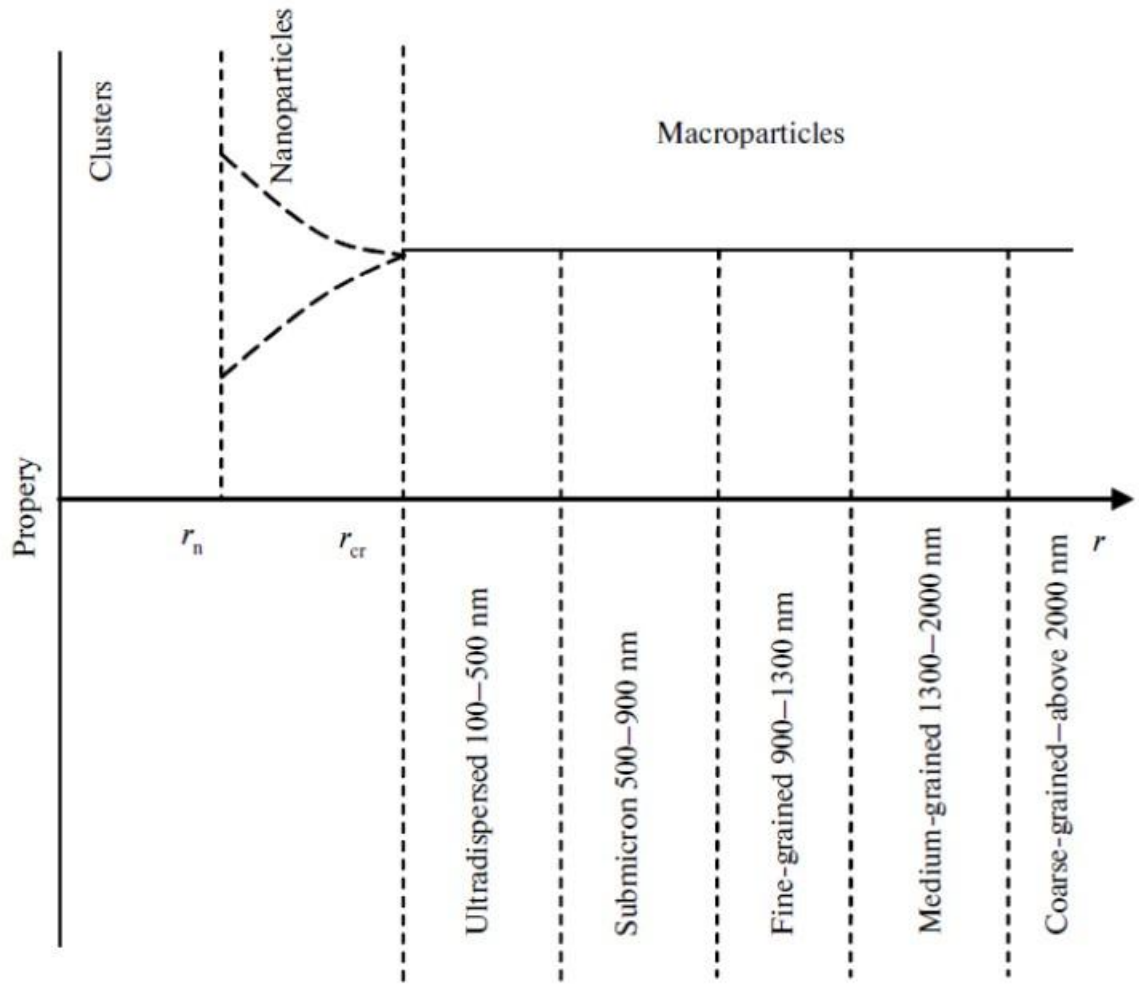

Figure 1: Classification of WC-Co particles by sizes after *[16]*

In cemented tungsten carbide, it has been well agreed that hardness of the cermet materials is inversely proportional to the grain size of material. Fracture toughness is always inversely proportional to hardness in cemented tungsten carbide, however this relationship between fracture toughness and hardness could not be linear whenever grain sizes are so fine. Then, finer grain size generally gives a lower fracture toughness. But, nanostructured metal alloys and ceramics is well-known that mechanisms are different of strengthening for sure due to the large volume fractions of grain boundaries. Deformation rely on diffusion controlled processes and the grain boundary sliding. In polycrystalline metals the grain boundaries also obstruct the cracks movements, this can

be say contributes to a well fracture toughness. By hypotheses, fracture toughness of this composite will be enhanced where WC grain sizes achieve nanoscale [18]. Table1 shows hardness and fracture toughness of nano scale WC bulk materials at different consolidation processes, for convenience of comparison, the original hardness values from papers were converted to Vickers hardness values and fracture toughness values was calculated from indentation method.

The most two important mechanical properties of cemented tungsten carbide and other cermets are fracture toughness and hardness. Such as wear resistance, flexural strength and impact resistance, as examples of other properties are basically dependent on fracture toughness and hardness [18]. Fracture toughness had been showed by data of sintered WC–Co using nanostructured powders that it decreases as the hardness increases [18]. Yu Milman [19] showed that in the temperature range **(**–196 to 1000°C), hardness of cemented carbides can be described by equation of the Hall Petch type, which makes it possible to find hardness at the known grain size and cobalt binder concentration. Also, in scratch tests [20] WC grain size plays a role in the wear mechanism, ultra-fine grades gave a limited slip compared to the coarser grades, and the smaller grain sized result in a better scratch resistance because it gives a lower scratch depth and width. P. Krakhmalev [21] investigated the influence of microstructural parameters of WC grain size on the edge wear mechanisms in series of WC–Co hardmetals finding that ploughing is the predominant operative wear mechanism since contact area exceeds the features of the microstructure and, therefore, stress is more homogeneously distributed into the bulk. Thus, a homogeneous behavior like ploughing is most likely to occur over all the sliding distances.

Table1 : Hardness and fracture toughness of sintered WC-Co by different consolidation processes using nano sized powders after *[18]*

Consolidation process	Sintered grain size (nm)	Hardness (Hv)	Fracture toughness(Mpa mm^0.5)
Hot pressing	**169**	**2084**	**8.8**
Hot pressing	**95**	**1100**	**14**
Hot pressing	**780**	**1575**	
SPS	**780**	**1725**	
HIP	**~400**	**1740**	
HIP	**~200**	**1910**	
SPS	**230**	**2030**	**13.5**
SPS	**800**	**1450**	**10.9**
SPS	**470**	**1570**	**11.42**
SPS	**280**	**1569**	**9.3**
SPS	**170**	**1726**	**9.5**
SPS	**200**	**2030**	
SPS	**<100**	**1887**	**11.5**
SPS	**~350**	**1800**	**12**
HFIHS	**323**	**1886**	**13.5**
PPS	**50**	**2250**	**15.3**
ROC	**0.15**	**1936**	**9.8**
UPRC	**~97**	**1845**	**10.2**

Larger WC grains materials like 20 µm and 30 µm exhibit ductility, but smaller grains of such powders like 3 µm and 6 µm are approximately brittle. In addition, Young's modulus was obviously as shown in Figure 2 an independent relation of the WC grain size. With about 577 GPa Young's modulus for the WC grains of 3 µm to 20 µm, 523 GPa Young's modulus for grain sizes of 30 µm as well [22].

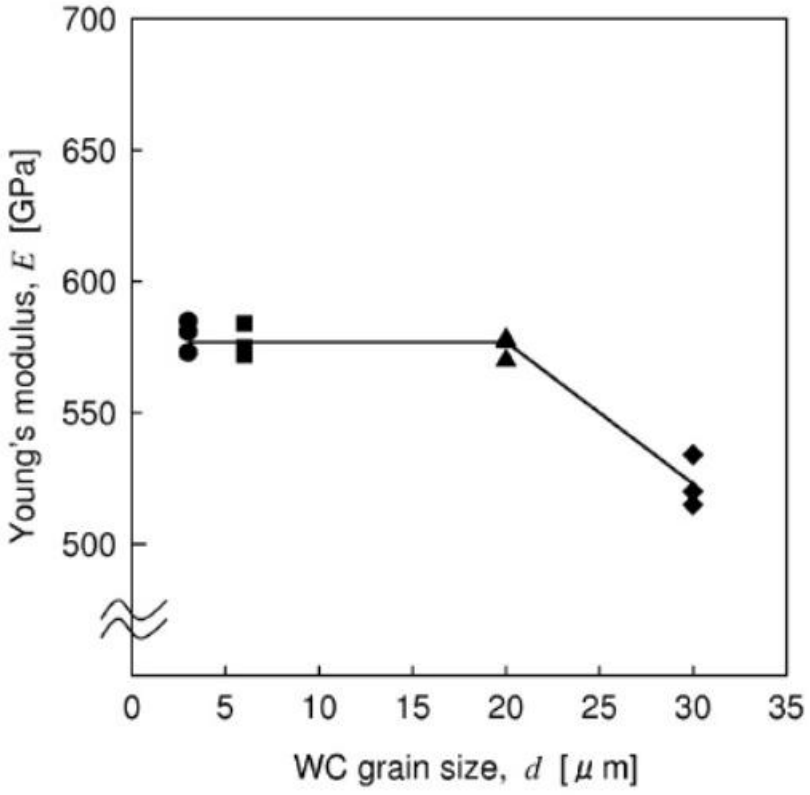

Figure 2: Young's modulus at different grain size of WC *[22]*

2.1.2 Effect of cobalt content

Cemented carbides used in technical applications normally contain between 5 to 25 wt. % cobalt. Stability and the strength of transfer film in order to withstand the sliding disorders depends on the cobalt binder phase ductility [23]. Cobalt's ductility helps formation of transfer film that is dense, which give a noble adherence under the dry sliding media [23]. Material's hardness decreases as cobalt content increases, while compressive strength can reach the maximum amount at 5 wt.% Co and then drops sharply when the cobalt content is increased [24]. On the other hand, the transverse rupture strength enhances with the increase of cobalt content reaching a maximum point at a cobalt content of approximately 20 wt.%. The composition that provides a maximum strength relies on other variables like the WC grain size [24]. In some cases, a maximum strength has been observed with a cobalt content greater than 30 wt. % [25]. The distribution of grain size and the

cobalt amount are the two major features which are affecting material removal rate and surface smoothness [26]. H. Saito et al [27] examined Co content of percent and WC grain size of the cemented carbide on the wear mechanism with a sum up that the wear increases with increasing of both WC grain size and Co content and that the same as [17]'s conclusion. Figure 3 shows a lower specific wear rate at lower size and cobalt content, Figure 4 shows that hardness decreases linearly at higher cobalt content at the same grain size and decreases with increasing grain size and Figure 5 shows that coefficient of friction scatters between 0.4 and 0.7 at different sizes and cobalt content. S. Ndlovu [20] investigated the scratch testing of cemented carbides and found that cobalt content influence the damage mechanism, the lower binder content of cobalt resulted in higher scratch resistance.

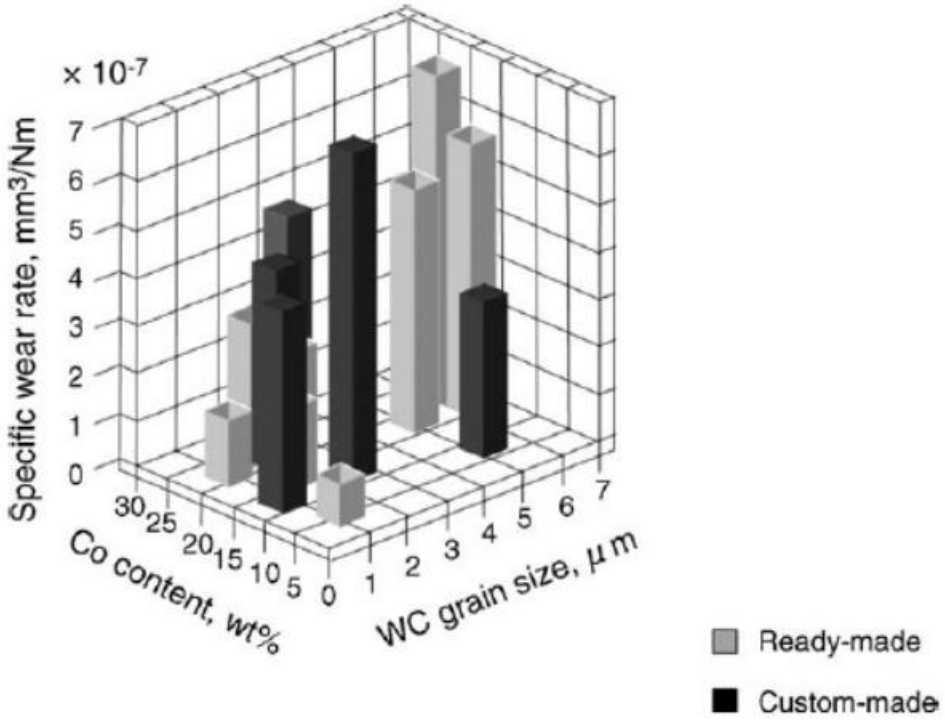

Figure 3: Graph showing map representation relationship between specific wear rate, Co content and grain size *[27]*

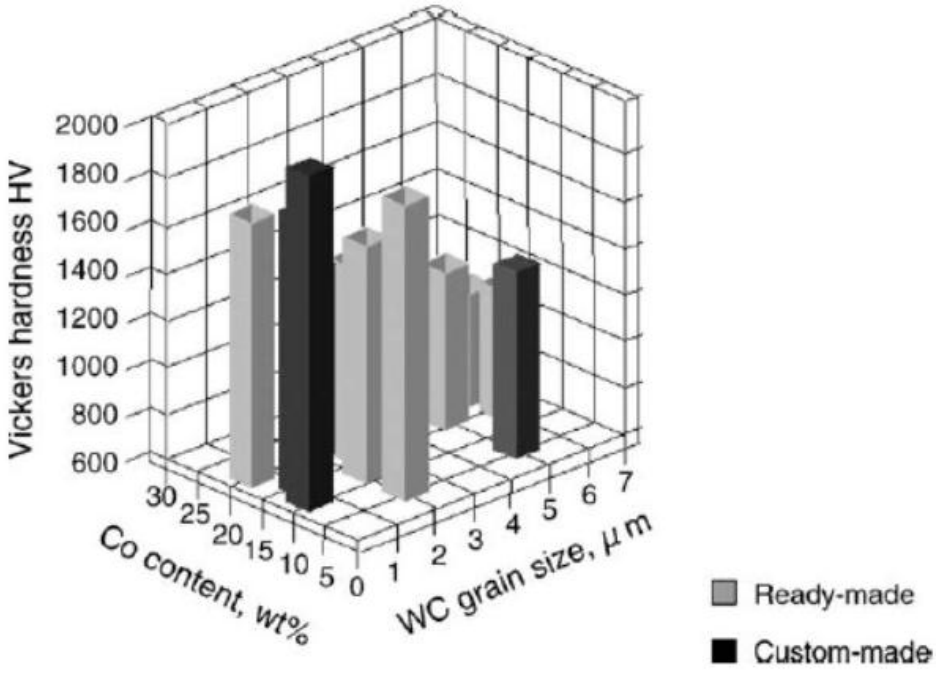

Figure 4: Graph showing map representation relationship between hardness, Co content and grain size *[27]*

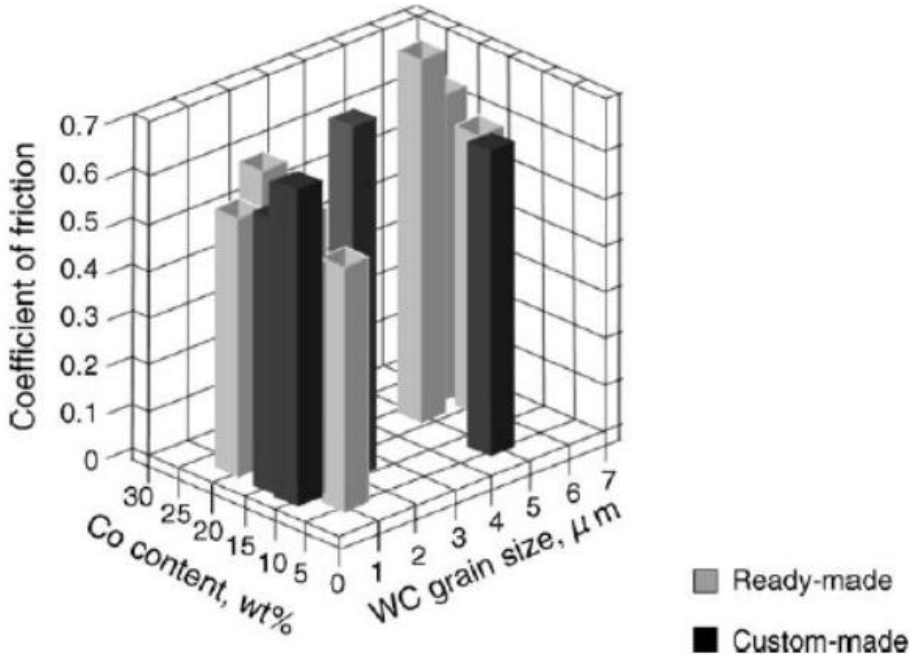

Figure 5: Graph showing map representation relationship between friction, Co content and grain size *[27]*

2.1.3 Effect of additives & inhibitors

A study was carried on WC–Co with Cr_3C_2–VC alloys finding that when we add Cr_3C_2–VC will result in decreasing friction of those alloys [28]. The sliding wear and friction had been explored by Pirso et al [29] they found that sliding wear and friction of WC–Co composite, Cr_3C_2–Ni composite and TiC–NiMo composite of cermets by means of modified block processed on a ring test. The one which depends on composition of such cermet of wear response was the Cr_3C_2–Ni cermets whereas other two of cermet grades were dependent on content of the binder in the composite. Adding to this, wear properties of WC–Co– (Ta, V) C alloy had been assessed by Quercia et al [30] under situations of sliding, erosion as well as abrasion settings. They ended up by concluding that wear response of that composites was rely on the mechanical properties and tribosystem configuration of that composites. By adding less than 1 wt. % TaC to the tungsten carbide alloy we will get outstanding increase in the sliding resistance of alloys wear [12] .And adding Cr_3C_2 and VC grain growth inhibitors will result in lowering the WC-Co eutectic onset temperature approximately by ~ 50°C [15]. Y. Pérez Delgado et al indicated that WC-10%Co (Cr/V) has giving us superior friction and reciprocating wear performance matching, or rather comparing with WC–10%Co alloy without no additions [26]. L. Espinosa-Fernández et al [31] showed that Cr_3C_2/VC grain growth inhibitors reduces the wear rates. N. Al-Aqeeli et al [32] found Cr_3C_2 is more effective to provide higher hardness and comparatively higher densification values and when we add 0.6 wt. % of the inhibitor it was proved to be a saturation point in 9 wt. % Co and VC was found to be more effective in restricting grain growth but with higher amounts showed more microporosity. Figure 6 shows the influence of amount and type of grain growth inhibitors, and amount of cobalt content and sintering temperature on Vickers hardness of nano cermets. T. Laoui and O. Biest [1] showed in detail the influence of adding TiC on tungsten carbide cermets

and they concluded that its addition enhances the toughness moderately and reduces the strength and hardness as well.

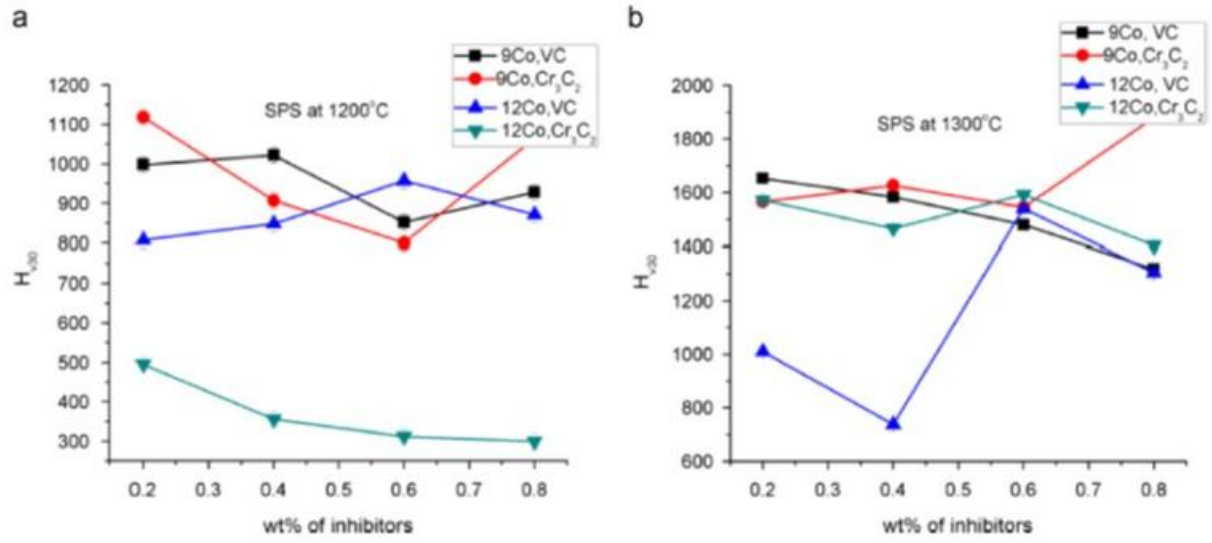

Figure 6: Effect of amount, type and sintering temperature of grain growth inhibitors on hardness at different content of inhibitor and Co content *[32]*

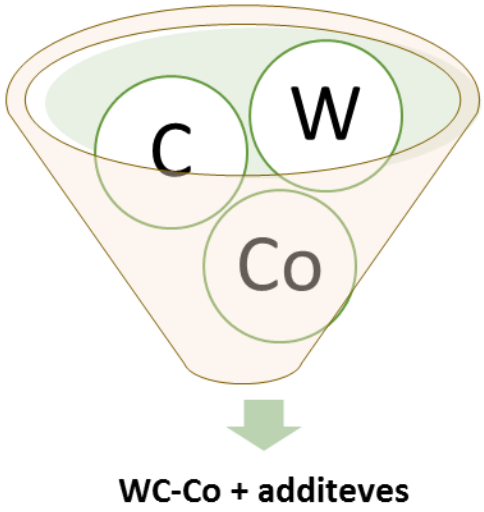

2.2 Effect of temperature

2.2.1 Tribological properties at room temperature

Friction coefficient values between the same tribopairs of the alloy WC–10%Co had been stated in literature by tests that had been done at the room temperature are contradictory slightly. Average of values comparably for the coefficient of friction of roughly 0.3 were recently stated for tungsten carbide samples that had been sintered by the spark plasma (SPS) [28]. By means of a pin on plate tribometer tests were applied on dry conditions by a sliding of a 6 mm WC–6wt. %Co pin on samples which are polished of WC–10%Co, with 0.10 m/s constant linear speed. And 30 N applied normal load. These conditions of tests yielded to 3.45 GPA Hertzian maximum pressure. Against WC– with 6%Co 5 mm ball radius, 40 N a normal load with sliding behavior at room temperature Espinoza et al. [33] examined WC–Co–Cr_3C_2–VC composite, they had got 0.35 average value. P_{max}, in static conditions of 3.12 GPa produced of the normal load of the maximum Hertzian pressure. Giving a result almost the same as found of wear test that employed through present investigation P_{max} = 3.10 GPa.

A reciprocating sliding test of like tribopairs had been carried out by Bonny et al. [34] applying a pin radius of 4 mm, 100 N load, getting 0.4 as an average coefficient of friction for a 5.95 GPa P_{max}. But, Casas et al. [35] showed findings that different than those publications. 1 friction coefficient at room temperature had been determined by a tribometer of pin on ring, these 4 mm of diameter pins of WC–10%Co were put in materials and examined with a sliding velocity of 0.5 m/s and normal load of 56 N yielding to 5.1 GPA maximum Hertzian contact pressure. Coarse grained and fine-grained samples had been evaluated with means of multiple and single scratch tests by J. Zunega et al [36] using a spherical stylus of diamond representing a creation on scratches' surfaces of a tribo layer. Y. Perez Delgado et al [37] carried out an experimental

evaluation of WC-Co hardmetal with investigation of friction and wear properties with a comparison of unlubricated rotating and linearly reciprocating sliding pairs at room temperature and they found that friction coefficient and wear levels are higher for unidirectional rotating sliding experiments against linearly reciprocating test conditions. A set of polished tungsten carbide based hard metal grade materials had been performed by K.Bonny et al. [38] in order to characterize behavior of wear by dry friction experiments at room temperature proving that the plate's wear is reported to be higher with growing of normal load and with lowering Vickers hardness, excluding for plate-pin system that has been identical, as the rate of wear is becoming higher value due to the more pronounced creation of a film adheres throughout friction. J. Pirso et al. [39] studied the friction and wear behavior of WC-Co hardmetals with different carbide grain size and different cobalt content at room temperature. Cobalt content was varied from 6 wt.% up to 20 wt.% along with carbide grain size increasing from 1µm to 1.5µm respectively. Friction and wear tests were conducted on block-on-ring tribometer under unlubricated conditions against steel disk at a normal load of 40 and 180N at sliding speed of 2.2m/s. Investigation of mechanical properties showed that hardness of WC-Co hardmetals decreased with increase in cobalt content while the rupture strength increased with increase in cobalt content. Volume loss and wear coefficient of hardmetal samples were found to be increasing linearly with increasing cobalt content. This increase was due to decrease in hardness with increasing cobalt content. Wear volume was also found to be increasing with increase in sliding distance, exactly according to Archard's equation.

Table 2: Review of literature for room temperature tribological testing for WC-Co hardmetals

Authors	**Title**	**Year of Publish**	**% of Co**	**Process**	**Size**	**Tribological Test**	**Test Type**	**Remarks**

K. Bonny Et Al. [28]	Impact of Cr_3C_2/VC Addition on The Dry Sliding Friction and Wear Response Of WC–Co Cemented Carbides	2009	6-10	Liquid Phase Sintering	Micro	Reciprocating Sliding Friction and Wear Behaviors under Unlubricated Condition	Pin-on-Plate	Cr_3C_2, VC Inhibitor
L. Espinosa Et Al. [33]	Friction and Wear Behavior Of WC–Co–Cr_3C_2–VC Cemented Carbides Obtained from Nanocrystalline Mixtures	2011	12	Liquid Phase Vacuum	40-80 nm	Friction and Dry Sliding Wear	Ball on Disc	Cr_3C_2/VC Inhibitor
K. Bonny Et Al. [34]	Friction and Wear Characteristics Of WC–Co Cemented Carbides in Dry Reciprocating Sliding Contact	2010	6-12		Sub-Micron	Unlubricated Reciprocating Sliding Wear	Pin-on-Plate	
J. Zunega et Al. [36]	Scratch Testing of WC/Co Hardmetals	2012	6-11		Micro	Single and Multiple Scratch Tests	Spherical Diamond Stylus	
Y. Delgado Et Al. [37]	Dry Sliding Friction and Wear Response of WC-Co Hardmetal Pairs in Linearly	2011	6-10	Liquid Phase Sintering	Micro	Dry Sliding Friction and Wear	Pin-on-Plate	A Comparison between Unlubricated

	Reciprocating and Rotating Contact							Rotating and Linearly Reciprocating
K. Bonny Et Al. [38]	Characterization of Tribological Behavior of Hardmetals		6-12		Sub-Micron	Dry Friction and Wear	Pin-on-Plate	Cr, V Inhibitors
Jüri Pirso et al. [29]	Friction and Wear Behavior of Cemented Carbides	2006	6-20	conventional	Micro	Sliding wear tests	Block on ring	
T. Kagnaya et al. [40]	Wear Mechanisms of WC–Co Cutting Tools from High-Speed Tribological Tests	2009	6.5		Micro	Dry Friction	Pin on Disc	

2.2.2 Tribological properties at elevated temperatures

Tools made of cemented carbide for high speed machines and dry cutting are in general the appropriate choice materials because of their pronounced resistance of heat and wear and for their hardness. About 600 °C of cutting temperature may be achieved during high speed machining or dry cutting by tools of the WC-Co cemented carbide, as a result of that wear and friction within tool and chip getting a higher amount, and this yield to wear rates with a much value, and thus, smaller tool lives [41]. Through a 0.6 µm to 2.2 µm WC average WC grain sizes range Deng Jianxin et al [41] studied the wear and friction behaviors of cutting tool materials of cemented carbide in an ambient air with 600 °C temperature, ball on disc system tribometer and they

concluded that a decrease in coefficient of friction as the test temperature increase as an indirect proportional relation Figure 7 and proved better performance at lower speed at different temperatures Figure 8. By sliding at 200 °C the coefficient gives its maximum value in their experiment, whereas the case of 600 °C exhibits the lowest value of coefficient of friction. Above this, the chief wear styles at temperature which are less than 200 °C were grain cracking and abrasion. In intermediate temperatures, the chief wear styles are grain pull out and wear due to the binder removal by the plastic deformation, at 600 °C temperature is the oxidative wear.

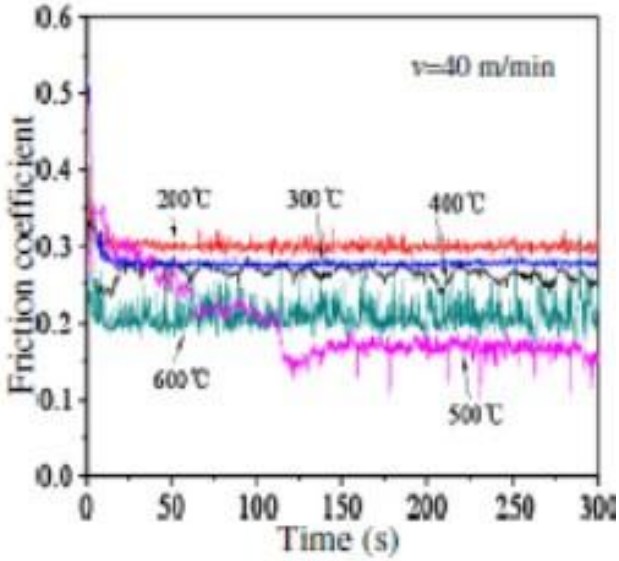

Figure 7: Variation of coefficient of friction at different elevated temperature of a micro sized WC-6%Co *[41]*

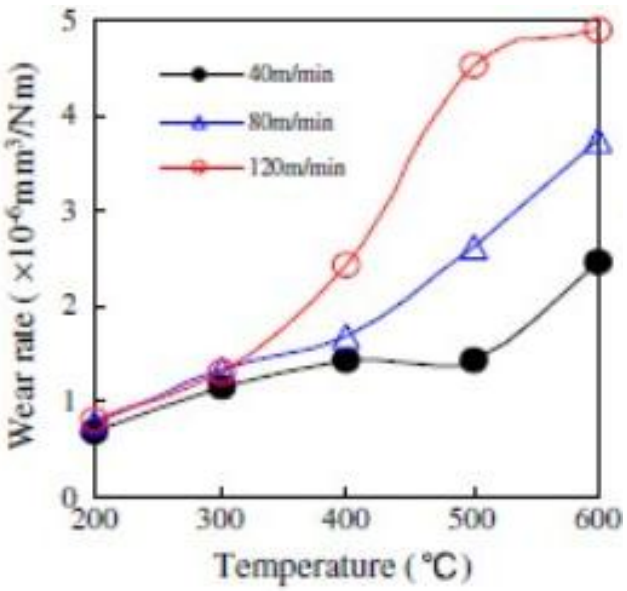

Figure 8: Wear rate variation of elevated temperatures with a different sliding speeds *[41]*

With increasing the test temperature, the residual stresses level will be lower slightly because of fabrication and preparation of sample at 400 °C temperature and this fact is the factor that we need to consider illustrating wear behavior [35]. Y. Pérez Delgado et al [26] studied WC–10%Co(Cr/V) alloy wear response and friction behavior with a plenty of surface finishes and they found that the wear rate by 400 °C are like 25 °C temperature findings, and this gives an indication that the temperature of the test has no an important effect.

Coatings of ultra-fine and nanostructured of cemented carbides with cobalt binder had been prepared by Hui Chen, et al [42] with a conclusion that the resistance of high temperature abrasion measurement of wear of nanostructured coating is preferred over ultra-fine. And, thermally sprayed of WC coatings with 12% cobalt had been studied by Q. Yang et al [43], they tested the behavior of sliding wear at high temperatures of 200 °C to 400 °C with high beta-cobalt and retention of WC proved that the exact rate of wear of these coatings is decreasing considerably with the increase of test temperature. To declare working efficiency and lifespan Xiaoliang Shi et

al [44], for a cutting tool material of an ultrafine WC cemented carbide with 10% cobalt binder composite, they reported that the cutting edge working temperature limit should be kept lower than 550 °C with no coolant in air.

E. Marui et al [45] investigated the wear characteristics of cemented carbides at an atmospheric temperature of 400 °C and confirmed that the wear is most influenced by the contacting surface temperature. Also, Hui Zhang et al. [46] observed the wear behavior of cemented carbides at elevated temperatures finding that the friction coefficient decreases with increase of temperature as well as increase the sliding speed. In contrast the wear rate increased with rather increasing operating temperature or sliding speed, but the speed did not have large influence on wear rate like operating temperature. T. Kagnaya et al [40] performed measurements of wear parameters and temperature to better understand the wear mechanisms of the WC–Co pins, concluding that as the sliding speed and the pin temperature increase, the friction coefficient decreases. The reason is either the debris circulation into the contact or increase of the contact surface temperature. Debris circulation indicates that higher the sliding speed the more the pin is worn; WC–Co particles are crushed to powder in the contact and participate to the friction as a third-body. The increase of temperature damages the mechanical properties of both pin and disc, particularly the disc ones. The temperature developments are resulting from the friction and from the circulation of debris in the contact too. The friction coefficient and the temperature curves always have the same up-growth versus test duration. The wear volume of the pin is directly depending on the mechanical energy dissipated in the pin. At low sliding speeds, the wear mechanisms of the pin are subjected to plastic deformation and micro-cracking of WC grains, fragmentation and de-bonding of WC grains and polishing of the pin contact surface. At high sliding speeds, a supplementary wear mechanism is observed. It deals with transfer of iron oxide. When iron transfer appears, the friction

coefficient and temperature curves versus test duration are very anarchic. The thermal power dissipated in the pin depends on the sliding speed.

Table 3: Review of literature for elevated temperature tribological testing for WC-Co hardmetals

Authors	Title	Year of Publish	% of Co	Process	Size	Test	Temperature Range °C	Test Type	Remarks
Xiaoliang Shi Et Al. [44]	Oxidation of Ultrafine-Cemented Carbide Prepared from Nanocrystalline WC–10Co Composite Powder	2008	10	Spray Pyrolysis-Continuous Reduction and Carbonization	Nano		450-700		
Deng Jianxin Et Al. [41]	Friction and Wear Behaviors of WC/Co Cemented Carbide Tool Materials with Different WC Grain Sizes at	2012	6	Conventional	Micro	Friction and Sliding Wear	Up To 600	Ball-on-Disk	

	Temperatures Up to 600 °C								
Y. Delgado Et Al. [26]	Influence of Wire-EDM on High Temperature Sliding Wear Behavior of WC10Co (Cr/V) Cemented Carbide	2013	10	Wire-EDM	Micro	Friction and Wear	25-400	Pin on Disk	Cr_3C_2/VC Inhibitor
Hui Chen Et Al. [42]	Research on The Friction and Wear Behavior at Elevated Temperature of Plasma-Sprayed Nanostructured	2009	17	Plasma Spray	Nano	Friction and Wear	600		Coatings

	WC-Co Coatings								
Q. Yang Et Al. [43]	Sliding Wear Behavior of WC–12% Co Coatings at Elevated Temperatures	2006	12	Thermal Spray	Micro	Dry Sliding Friction and Wear	Up to 400	Ring on Plate	Coatings
E. Marui, H. Endo and A. Ohira [45]	Wear Test of Cemented Tungsten Carbide at High Atmospheric Temperature (400 _C)	2000	6.5	powder metallurgy	Micro	Dry Sliding	400	Pin on Disc	(TiC) & (TaC) added

Hui Zhang et al. [46]	Effect of Ambient Temperature on Wear of Cemented Carbide Tool Material	2011	6-8		Micro	Dry sliding	200-600	Ball on Disc	TiC addition tested

Summary

From the literature above we find that there is a need to study the wear and friction on bulk and dense WC- Co. Primarily, evaluation of wear rate at two different particle sizes of WC (Micro & Nano) and comparing the performance at different speeds, different loads and at a range of temperatures. Thus, to evaluate the effect of Micro and Nano particle sizes of WC at high loads and elevated temperatures on the wear rate and understanding the underlying wear mechanisms throughout those conditions becomes very significant, which is the focus of the present study.

CHAPTER 3

3. FABRICATION & CHARACTERIZATION

3.1 Material preparation

3.1.1 Raw materials

The starting powder materials which are used in this study are tungsten carbide (WC) with an average particle size of 3.5 µm as hard base material and cobalt (Co) with an average particle size of 1.5 µm as the soft binding material. Both materials were procured from William Rowland limited, UK.

3.1.2 Sample fabrication

Samples of cylindrical geometry (20mm diameter X 6mm) were fabricated using a two-step process of high energy ball milling for uniform mixing of the powders followed by spark plasma sintering (SPS) process for consolidation.

i. Milling and Mixing

All milling and mixing operations were carried out using a High-Energy ball mill (Model HSA-1, UNION PROCESS, USA) which is shown in Figure 9. The as received WC powder of 3.5 µm was milled to achieve the required nano size WC powder using the HDDM mode for 5 hours at 2000 rpm using Zirconia balls of diameter 0.6 mm. HDDM mode is used for higher than 1000 rpm and wet milling medium. Powder to balls ratio used was 1:20 in a medium of ethanol to keep the procedures clean, homogenous and uniform. During milling, at different intervals, powder samples were taken from each vial to be analyzed through scanning electron microscope (SEM) and Field Emission Scanning electron microscopy (FESEM). Analysis was carried out to get the change in

morphology of the powders and micro structure, as an effect of the milling time, using a secondary electron mode at an accelerating voltage of 30 kV. Gold coatings over those powders were applied to improve conductivity and resolution of micro structural images. Energy Dispersive X-ray (EDX) spectroscopy was used to confirm compositions and purity of these samples.

Mixing parameters to obtain a homogeneous mixture of WC-9%Co for both micro and nano size mixtures are shown below in

	%Co	RPM	Ball Material	Size	Powder to ball Ratio	Time
3.5 µm WC	9	200	WC	6 mm	1:5	1 h
100 nm WC	9	200	WC	6 mm	1:10	3 h

Table *4*. Cobalt powder had been added to both processes, mixing of micron and nano sized WC, at the beginning of each procedure and lasts the whole time of mixing to allow homogenous mixing procedure. Adding 9 wt.% of cobalt to cemented carbides showed hard and dense samples for both sizes of WC prepared by spark plasma sintering (SPS) [47]

	%Co	RPM	Ball Material	Size	Powder to ball Ratio	Time
3.5 µm WC	9	200	WC	6 mm	1:5	1 h
100 nm WC	9	200	WC	6 mm	1:10	3 h

Table 4: Mixing parameters using ethanol medium for both sizes of WC with the Co content

Figure 9: High energy ball mill (model HSA-1), KFUPM, Dhahran.

ii. Sintering procedures

Mixtures were dried at room temperature for 24 hours ensuring complete evaporation of ethanol. Spark plasma sintering (SPS) (HP D-50 type, FCT System, Rauenstein, Germany) shown in Figure 10 was carried out using graphite dies.

WC size	**3.5 µm**	**100 nm**
Sample dimensions (mm)	Diameter: 20; Thickness: 6	Diameter: 20; Thickness: 6
Pressure (MPa)	45	50
Holding time (min)	10	10
Temperature (ºC)	1200oC	1250oC
Heating Rate (ºC/min)	100	100

Atmosphere	Vacuum	Vacuum

Table 5 shows the sintering parameters for the micron and nano sized WC samples mixed with 9wt% Co. The sintering parameters were optimized by conducting preparing numerous samples and analyzing them in terms of densification, porosity and micro structure. Spark plasma sintering (SPS) was carried out in vacuum at 100 ºC/min heating rate and 10 minutes holding time. The optimized sintering pressure and temperature for the micron sized mixture of WC - 9%Co were 45 MPa and 1200 ºC. For the nano sized mixture of WC - 9%Co the optimized sintering pressure and temperature were 50 MPa and 1250 ºC respectively.

WC size	**3.5 µm**	**100 nm**
Sample dimensions (mm)	Diameter: 20; Thickness: 6	Diameter: 20; Thickness: 6
Pressure (MPa)	45	50
Holding time (min)	10	10
Temperature (ºC)	1200ºC	1250ºC
Heating Rate (ºC/min)	100	100
Atmosphere	Vacuum	Vacuum

Table 5: Optimized sintering procedures for both sizes of WC, 3.5 µm WC at (45 MPa, 1200ºC) and 100nm at (50 MPa, 1250ºC)

Figure 10: Spark plasma sintering (SPS) (HP D-50 type), KFUPM, Dhahran

3.2 Characterization techniques

3.2.1 Surface preparation

All sintered samples were mounted using a Buehler transoptic powder with a polymer pressed in a hot press (Evolution, IPA 40 Remet, Bologna, Italy) at 200 C for 30 minutes to complete the entire process. However, it is to be noted that this polymer had been removed for the wear tests at elevated temperatures. The samples were grinded and polished by (Buehler Magno-discs, USA) using 125, 74, 40, 20 and 10 µm diamond grinding sheets using water as a medium followed by a smooth polishing using Buehler diamond suspension of 3 µm to obtain an average surface roughness (R_a) value of approximately 0.11 ± 0.01µm for the micron samples and (R_a) value of 0.17 ± 0.02µm for the nano samples.

3.2.2 Density measurements

Density of the samples was measured by using MD-300S, Alfa Mirage, SG resolution-0.001g/cm^3, capacity-300g densimeter based on the Archimedes principle. Density measurement plays an essential role in qualifying the sintered samples. A typical way to evaluate the density is to use the rule of mixture to evaluate the theoretical density, and thereafter the densification, through the consideration of the individual densities of the resultant phase and their weight ratios after sintering. Equation 1 represents the general formula to calculate the density for the sintered samples.

Equation 1

$$\rho = \frac{A}{A-B}(\rho_0 - \rho_L) + \rho_L$$

$$\rho_L = 0.0012\ g/cm^3$$
$$\rho_0 = 1\ g/cm^3$$

A and B represent the weight of sample in air and liquid, respectively. ρ_o is the liquid density which is water in our case, while ρ_L stands for air density. Units of weights is in grams and density in g/cm^3.

3.2.3 Hardness Measurement

Vickers hardness (HV_{30}) was measured by the universal hardness testing machine (Zwick-Roell, ZHU250, Germany) using a load of 30 kg. The hardness tester was provided with a diamond indenter of pyramid shape and was used to obtain the depression on the samples. Vickers hardness can be calculated in GPa using the following formula

Equation 2

$$HV_{10} = \frac{1.854}{d^2} \ (9.81 \times 10^{-3})$$

Observed density and hardness for the 3.5 µm WC were 13.77 (g/cm^3), 93.9% densification, and 1411 (Hv_{30}), while the observed density and hardness for the 100 nm WC were 13.62 (g/cm^3), 92.8% densification, and 1495 (Hv_{30}).

3.2.4 Microstructural Analysis

Samples were coated by a thin layer of gold (9nm) by a sputter coater *(Model Q150T, Quorum Technologies, UK)* for SEM imaging. Scanning electron microscope (*FESEM, Lyra 3, Tescan, Czech Republic*) was used to characterize the samples. The electron gun voltage was varied between 20-30 KeV to get the best possible contrast. Both secondary and backscattered imaging modes were utilized in this study. An accompanied energy dispersive spectrometer (*EDS, Oxford Inc., UK*) was of great help in linking the EDS phases with their corresponding morphologies.

3.3 Tribological Testing

3.3.1 Wear Test

Wear testing of samples was performed on a Tribometer (UMT TriboLab, BRUKER, Germany) (Figure 11) with a ball on disc configuration at room temperature and elevated temperatures using an alumina ball (6.3 mm diameter, HV = 1707) as the counterface. Samples were grinded and polished to a surface roughness (R_a) 0.11 ± 0.01µm for the micron samples and (R_a) value of 0.17 ± 0.02µm for the nano samples, and subsequently cleaned with acetone and dried properly before each wear test. Wear tests were carried out for a sliding distance of 500 m with a track radius of 3 mm. Minimum of three runs of wear tests were performed and the average values of the coefficient

of friction and specific wear rates are reported. Table 6 shows the matrix of all the wear tests performed in this work and it is to be noted that each test was performed three times. After every test, optical images of the counterface ball were taken to analyze the wear on the ball during the sliding test.

For the wear tests at elevated temperatures, a sample fixture made of H-13 tool steel was fabricated to hold samples. The high temperature module of UMT-3 tribometer is provided with an insulated chamber to assure that the test temperature was kept constant during testing.

Table 6: Matrix of wear tests at different normal load, different sliding velocity, different environment temperature and each test performed three times.

Size	**load(N)**	**Speed(m/s)**	**temperature. (˚C)**	**Radius(mm)**	**Distance(m)**
micro WC	**15**	**0.1**	**RT**	**3**	**500**
micro WC	**30**	**0.1**	**RT**	**3**	**500**
micro WC	**45**	**0.1**	**RT**	**3**	**500**
micro WC	**30**	**0.2**	**RT**	**3**	**500**
micro WC	**30**	**0.4**	**RT**	**3**	**500**
nano WC	**15**	**0.1**	**RT**	**3**	**500**
nano WC	**30**	**0.1**	**RT**	**3**	**500**
nano WC	**45**	**0.1**	**RT**	**3**	**500**
nano WC	**30**	**0.2**	**RT**	**3**	**500**
nano WC	**30**	**0.4**	**RT**	**3**	**500**

micro WC	**30**	**0.1**	**300**	**3**	**500**
nano WC	**30**	**0.1**	**300**	**3**	**500**
micro WC	**30**	**0.1**	**600**	**3**	**500**
nano WC	**30**	**0.1**	**600**	**3**	**500**

Figure 11: Tribometer (UMT TriboLab, BRUKER, Germany), KFUPM, Dhahran

3.3.2 Optical Profilometry

After the wear tests, the wear track was examined under an optical profilometer (Contour GT-K Automated, BRUKER, Germany) (Figure 12) to measure the wear track depth and the wear track area to obtain the wear volume to calculate the specific wear rate using the below mentioned equations (Equation 3,Equation 4). A total of nine measurements were taken on each of the wear

tracks and the average value was used to calculate the wear rate. After every run, optical images of the counterface ball were taken to analyze the wear on the counterface ball during the test.

$$V = 2\pi * width * Area$$ Equation 3

$$SWR = \frac{V}{LOAD * DISTANCE}$$ Equation 4

Volume (V) represents the volume of the worn material for each sample, SWR represents the specific wear rate which is the volume divided by load times the sliding distance.

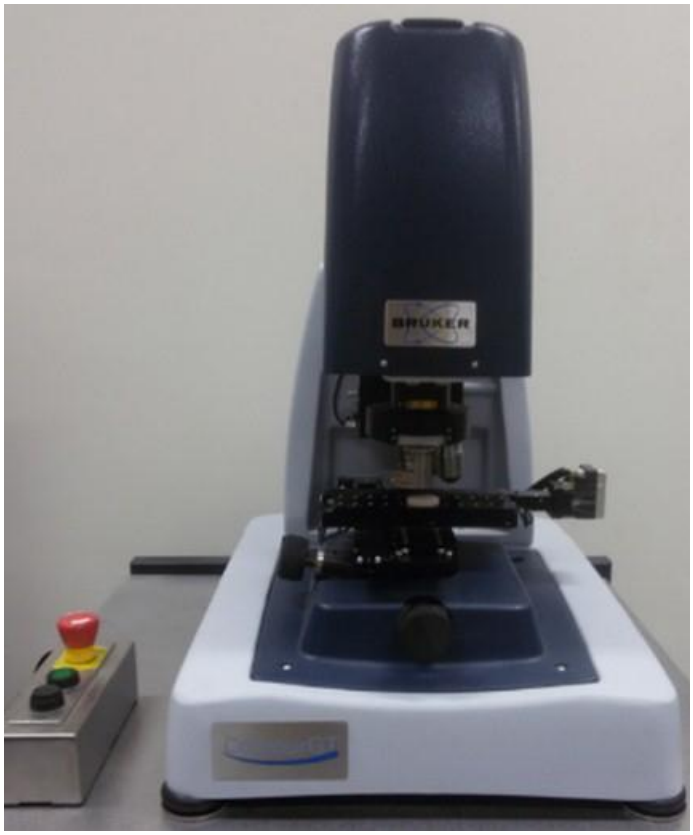

Figure 12: Profilometer (Contour GT-K Automated, BRUKER, Germany) KFUPM, Dhahran

3.3.3 Oxidation Analysis

Thermal gravimetric analysis of the samples was conducted at 600^0C in air by (TGA - STA 449F3 – Jupiter, NETZSCH, GERMANY) (Figure 13) then a qualitative/quantative x-ray diffraction (XRD) analysis was carried out under (MiniFlex II, Rigaku, JAPAN) (Figure 14) to understand the wear mechanisms.

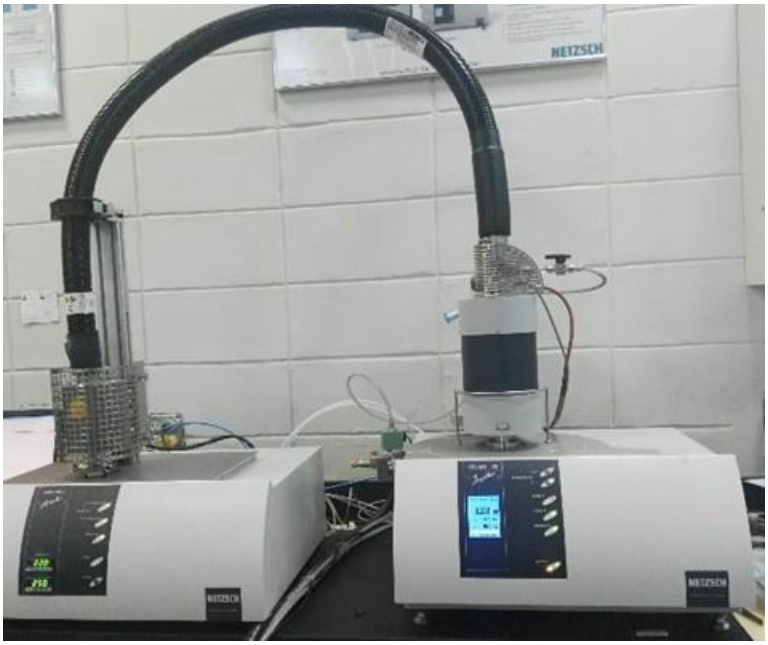

Figure 13: TGA (STA 449F3 – Jupiter, NETZSCH, GERMANY), KFUPM, Dhahran.

Figure 14: XRD (MiniFlex II, Rigaku, JAPAN), KFUPM, Dhahran.

3.4 Design and Fabrication of various fixtures

3.4.1 Grinding Sample Holder

Grinding and polishing of cemented carbides requires more time and more efforts especially the nano sized WC samples. Also, the small diameter of samples (20 mm) was a tough job during the experimental work. The automated grinder could not be used to grind and polish samples without mounting them by using the polymer. So, a design to hold the samples by hand was urgently needed and it was manufactured in the university's workshop as shown in Figure 15.

Figure 15: Sample holder for hand use to grind and polish samples.

3.4.2 Ball Holder

The need for a ball holder that can resist a high temperature of 300°C, maximum loads of 45N and speeds of maximum 0.4m/s during tests was a challenge. A design and manufacturing of a ball holder was carried out throughout this work. Design was based on high factor of safety to assure that the balls can be fixed during tests without any internal rotation. Figure 16 shows the ball holder that was fabricated at the university's mechanical shop.

Figure 16: Ball holder fabricated to hold ball of 6.3mm diameter during tests

3.4.3 High Temperature Sample Holding Fixture

The challenge during this work was to choose a material that can sustain high temperatures of 600°C. In addition, this type of material should be well designed to hold the samples tightly during the testing of samples at temperatures of 600°C and beyond, high loads and high speeds. H-13 tool steel material was chosen for its high resistance to corrosion at elevated temperatures and its high hot hardness. Fabrication of fixture (Figure 19) contains a base (Figure 17), two V shape sliders (Figure 18) to grip the samples and bolts were designed, fabricated and hardened at the university's mechanical shop. Hardening procedure of fixture's parts was in three stages. Firstly, holding the fabricated parts at 850° C for 20 minutes followed by heating at a rate of 10° C/min up to 1050° C and holding at this temperature for 30 minutes and lastly quenching the parts to room temperature.

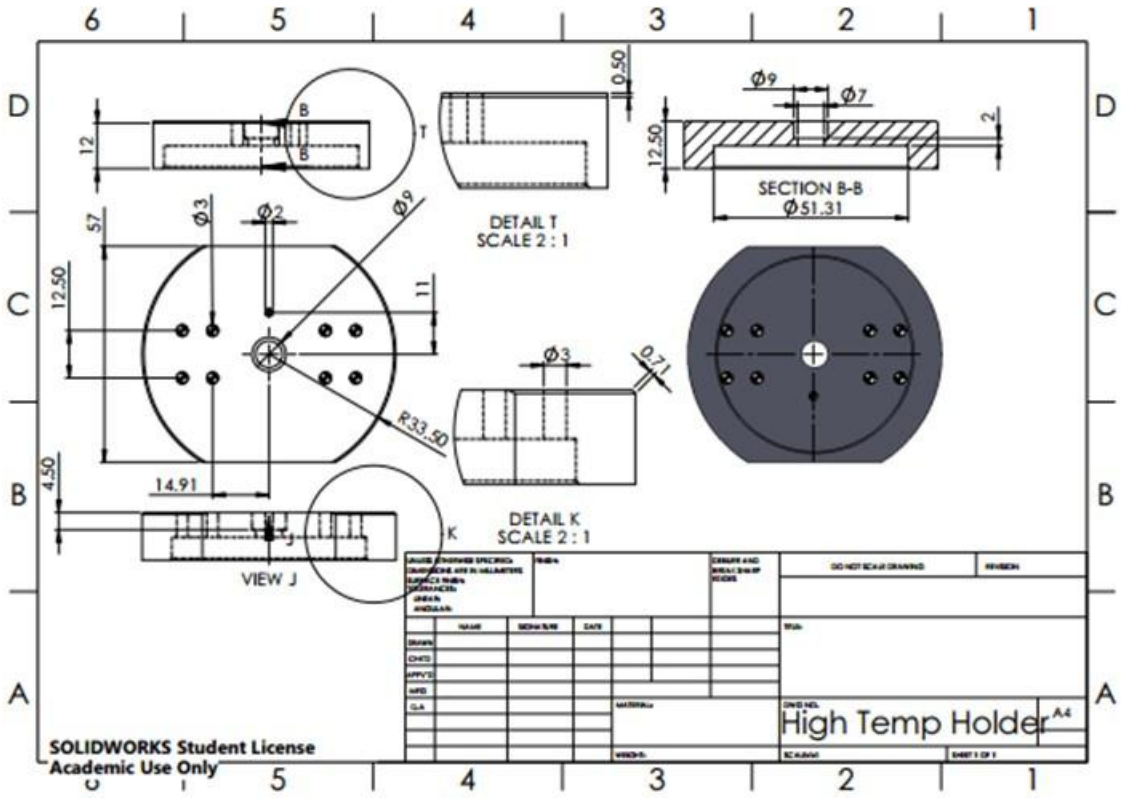

Figure 17: Base of the sample fixture to hold the WC-Co samples at elevated temperature tests

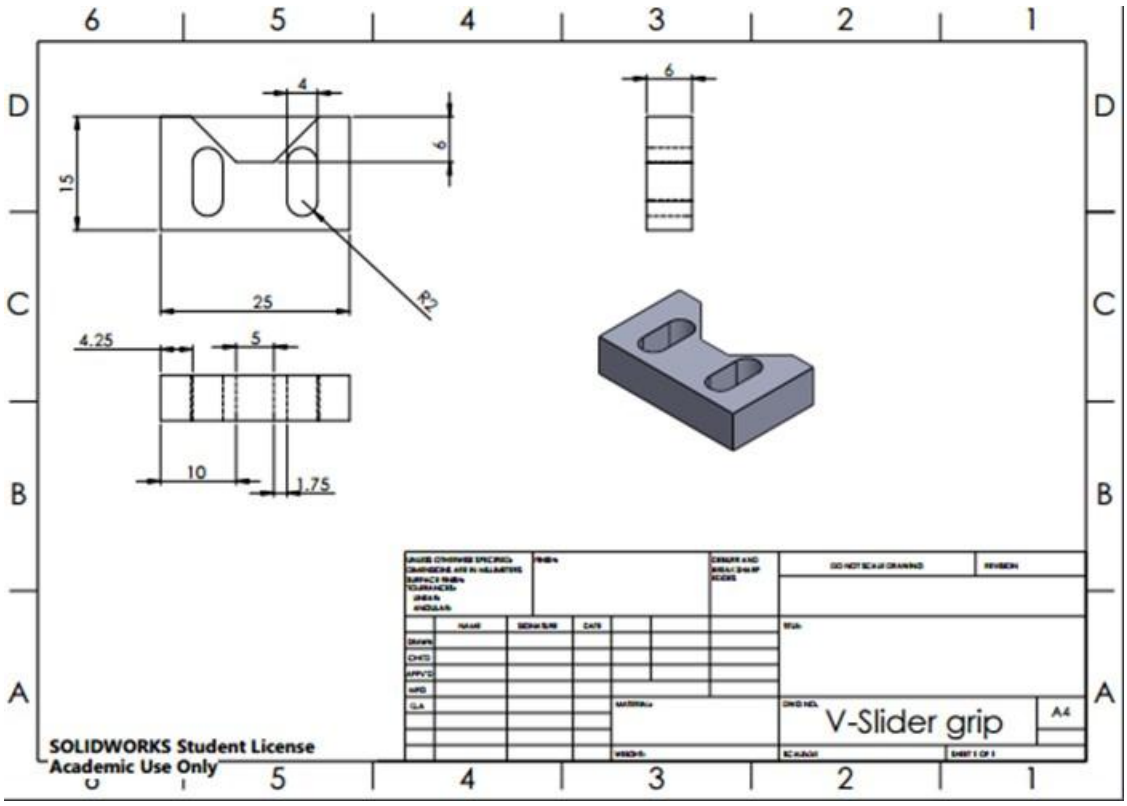

Figure 18: V slider grip of sample fixture and two grips were used to hold round samples

Figure 19: High temperature holding fixture of two V grips and four bolts

CHAPTER 4

4. RESULTS & DISCUSSION

4.1 PHASE I: Development and Characterization of The Micron Sized and Nano Sized WC-9wt%Co Composites Using Spark Plasma Sintering Technique

4.1.1 Surface Morphology

Figure 20(a) shows the SEM image of as received tungsten carbide with an average size of 3.5 µm. Figure 20 (b) shows the milled tungsten carbide whereby a significant reduction in the average particle size from 3.5 µm to 100 nm can be observed. Figure 20 (c,d) shows the optical microscope images of sintered WC-9Co samples for micro and nano size respectively. A uniform distribution of cobalt (dark regions) with tungsten carbide can be observed for both sizes.

From the Back scattered emission (BSE) images of SEM after sintering as shown in Figure 21, (a,b) for different magnifications (10k, 50k),the cobalt can be seen distributed with WC in micro sized samples, while Figure 21, (c, d) also show the nano sized samples at magnifications (20k, 100k) whereby the cobalt is uniformly distributed with no agglomeration which proves that the mixing and sintering procedures of the samples used in this study results in a homogeneous mixture and good scattering of 9% of Cobalt, and synthesis procedures exhibit similar achievement in [47]. The mechanical properties are known to be anisotropic in the WC-Co because of the crystallographic structure of WC hardmetals [24], this anisotropy is related to the resulted and optimized mechanical properties of samples and well distribution of matrix through hard phase.

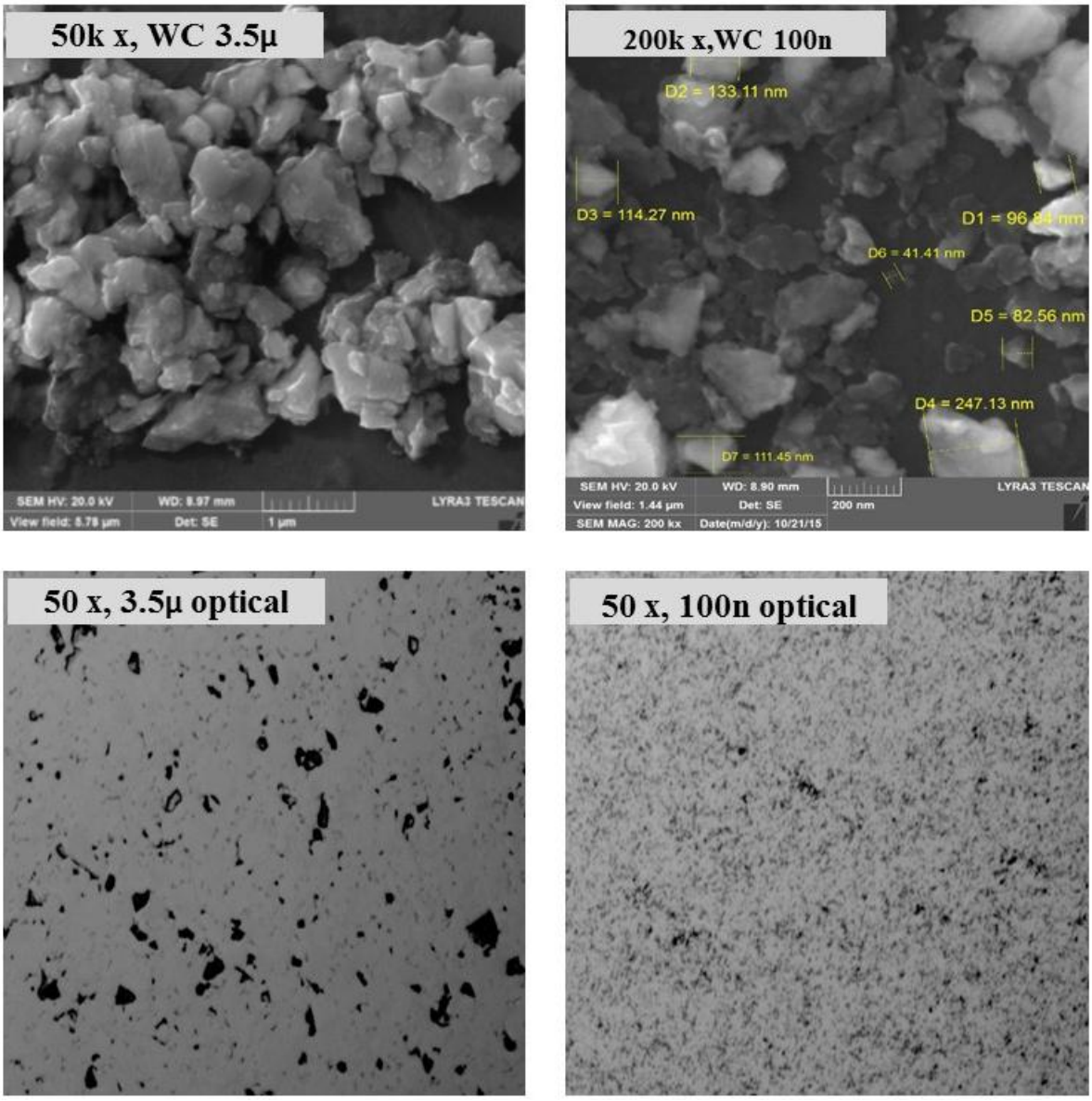

Figure 20: a) SEM image of the starting powder of WC, b) SEM image of milled WC reaching an average of 100 nm, c) Optical image of sintered sample of micron size, d) Optical image of sintered sample of nano size.

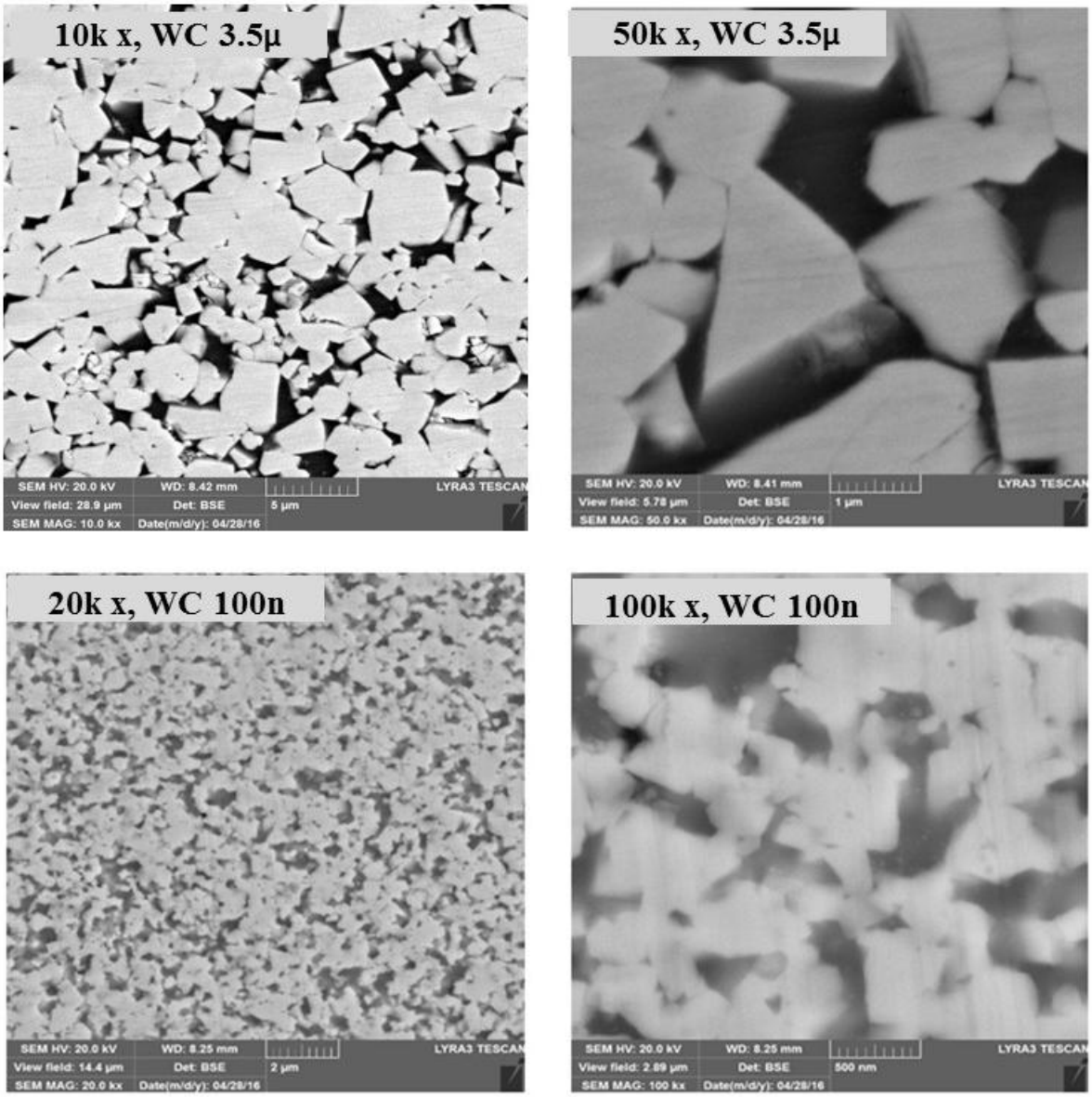

Figure 21: BSE SEM images of sintered samples by SPS a,b) 3.5µmWC-9%CO at (45MPa, 1200^{o}C), c,d) 100nmWC-9%Co at (50MPa, 1250^{o}C).

4.2 PHASE II: Tribological Characterization at Room Temperature

4.2.1 Effect of Load on the coefficient of friction and wear rate

Figure 22 shows specific wear rates for the micron size WC and the nano size WC samples tested at different loads (15, 30 and 45 N) at a constant linear speed of 0.1m/s for a sliding distance of

500 m under dry conditions at room temperature. It can be observed that at all the loads, the specific wear rates of the nano sized WC hardmetal showed lower wear rate as compared to the micron sized WC hardmetal, signifying an improved wear resistance with a reduction in particle size. This can be attributed to the fact that as the particle size of WC reduces, the effective surface area for bonding with the soft binder (cobalt) increases which in turn increases the hardness leading to a significant improvement in the resistance to the material pull out or wear.

An increase in the specific wear rates can be observed with normal load. However, a very sharp increase in the wear rate can be seen for the micron sized samples as load increases from 30 N to 45 N signifying the low resistance to material pull-out at higher loads. At a normal load of 15N, wear rates for the nano and micron sized samples is almost the same which can be an indication that at lower loads, the particle size of tungsten carbide has negligible effect on the wear rate. Figure 23 presents the variation of coefficient of friction (COF) with WC particle size and normal

load. It is observed that the COF increases for both the micron sized and nano sized WC samples with an increase in load.

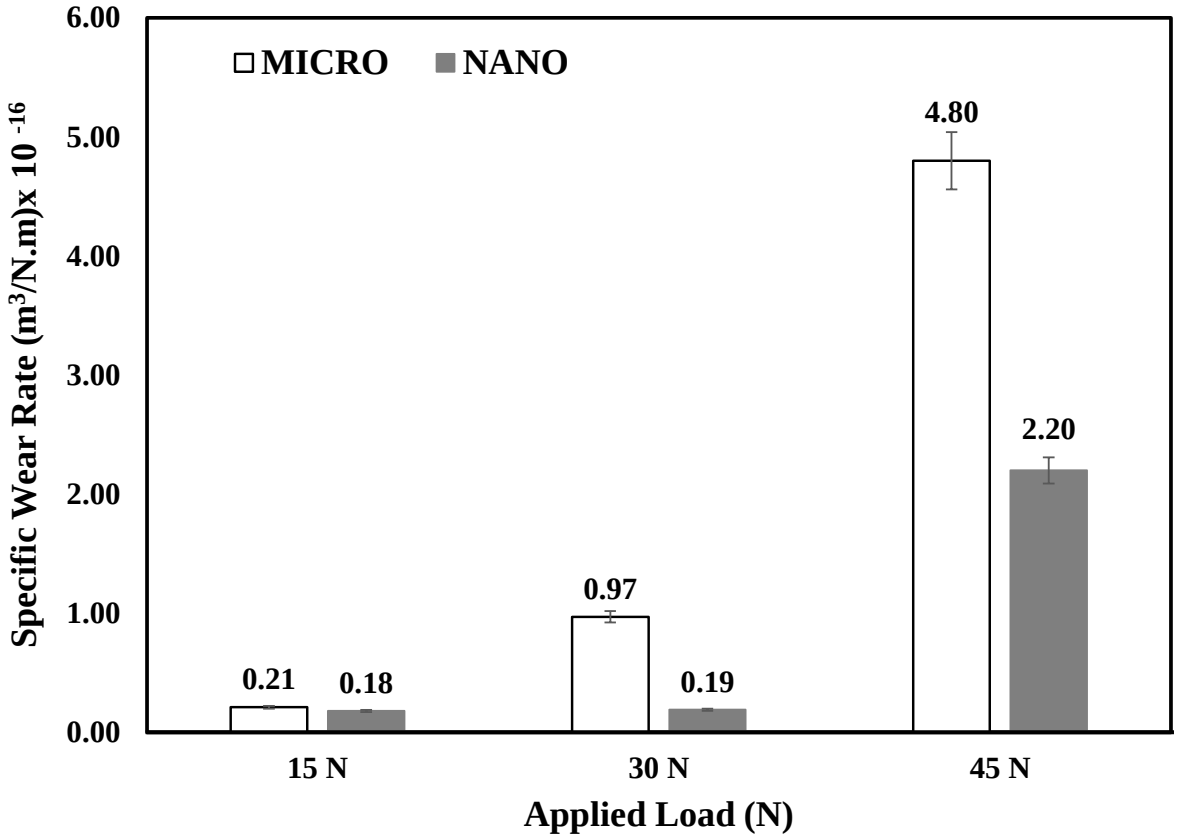

Figure 22: Variation of specific wear rate with WC particle size and normal load at a constant sliding velocity of 0.1 m/s under dry conditions at room temperature

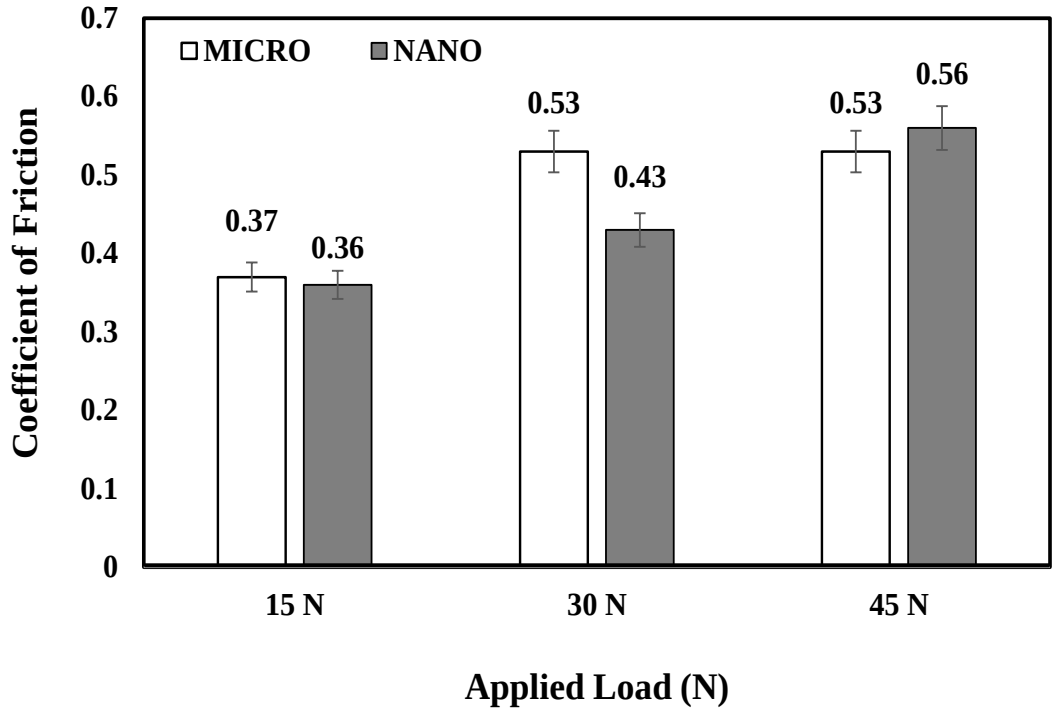

Figure 23: Variation of coefficient of friction of micro and nano sized WC samples as a function of particle size and normal loads at constant sliding velocity of 0.1 m/s under dry conditions at room temperature

Figure 24 and *Figure 25* summarize the wear track characteristics for micron size and nano size WC samples respectively at different loads of 15, 30 and 45 N. Wear tracks were analyzed using SEM imaging followed by 2-D optical profiling of each wear track at different locations. It can be observed from the 2D wear track profile images in *Figure 24* and *Figure 25* that, as the load increased the wear track depth increased leading to an increase in the specific wear rate in both the micron sized and nano sized WC samples. Optical images of alumina counterface after the wear tests done at different loads for both micron and nano sized samples are also shown in *Figure 24* and *Figure 25* respectively. It can be observed that as the load increased the wear scar mark on the counterface balls also increased suggesting a higher wear of the alumina ball. However, the wear

scar mark was observed to be lower in the case when the ball was sliding against the nano sized samples as compared to when sliding against the micron sized samples signifying the fact that smaller particle size results in lower wear. It can also be seen from the SEM images of the wear tracks (*Figure 24*) and the EDS mapping conducted on the wear track (*Figure 26*) that, in case of the micron sized WC samples, a lot of wear debris consisting of a mixture of alumina and WC is present on the wear track. This indicates that the predominant wear mechanism by which these samples wore out was abrasive wear by brittle fracture whereby the WC samples are easily broken out/pulled out of the soft binder because of poor bonding between them leading to higher wear.

However, when the wear tracks for the nano sized samples were investigated as shown in *Figure 25* and *Figure 26* respectively, the SEM images showed smooth wear tracks with hardly any debris material on the wear track suggesting that the predominant wear mechanism might be abrasive

wear due to plastic deformation. This can be attributed to the improved bonding between the hard and the soft phases in the nano sized WC samples due to an increase in the effective surface area.

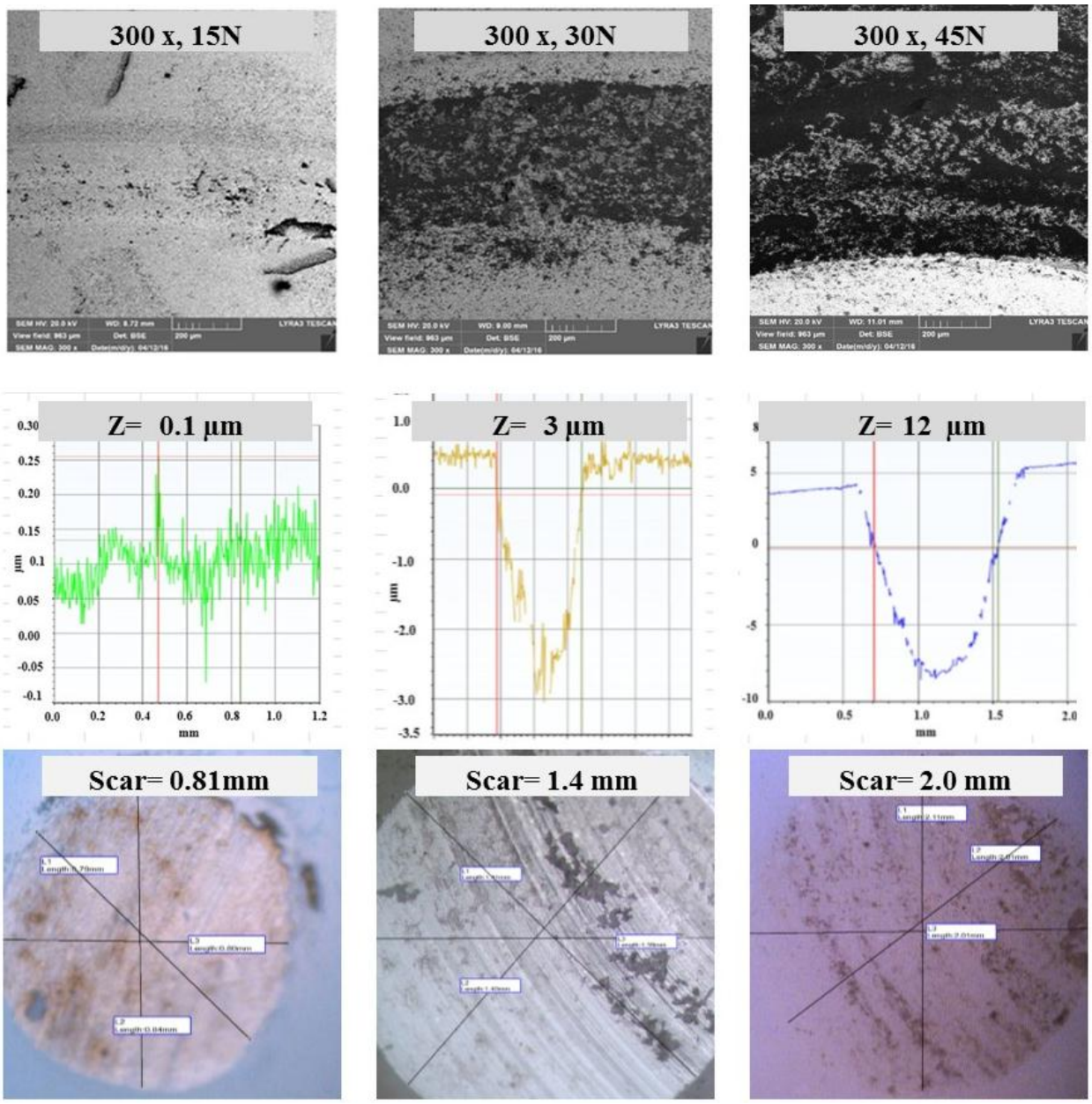

Figure 24: Summary of results of the micron size tests at different loads, each SEM image is related to a 2-D profile and scar mark of counterface ball

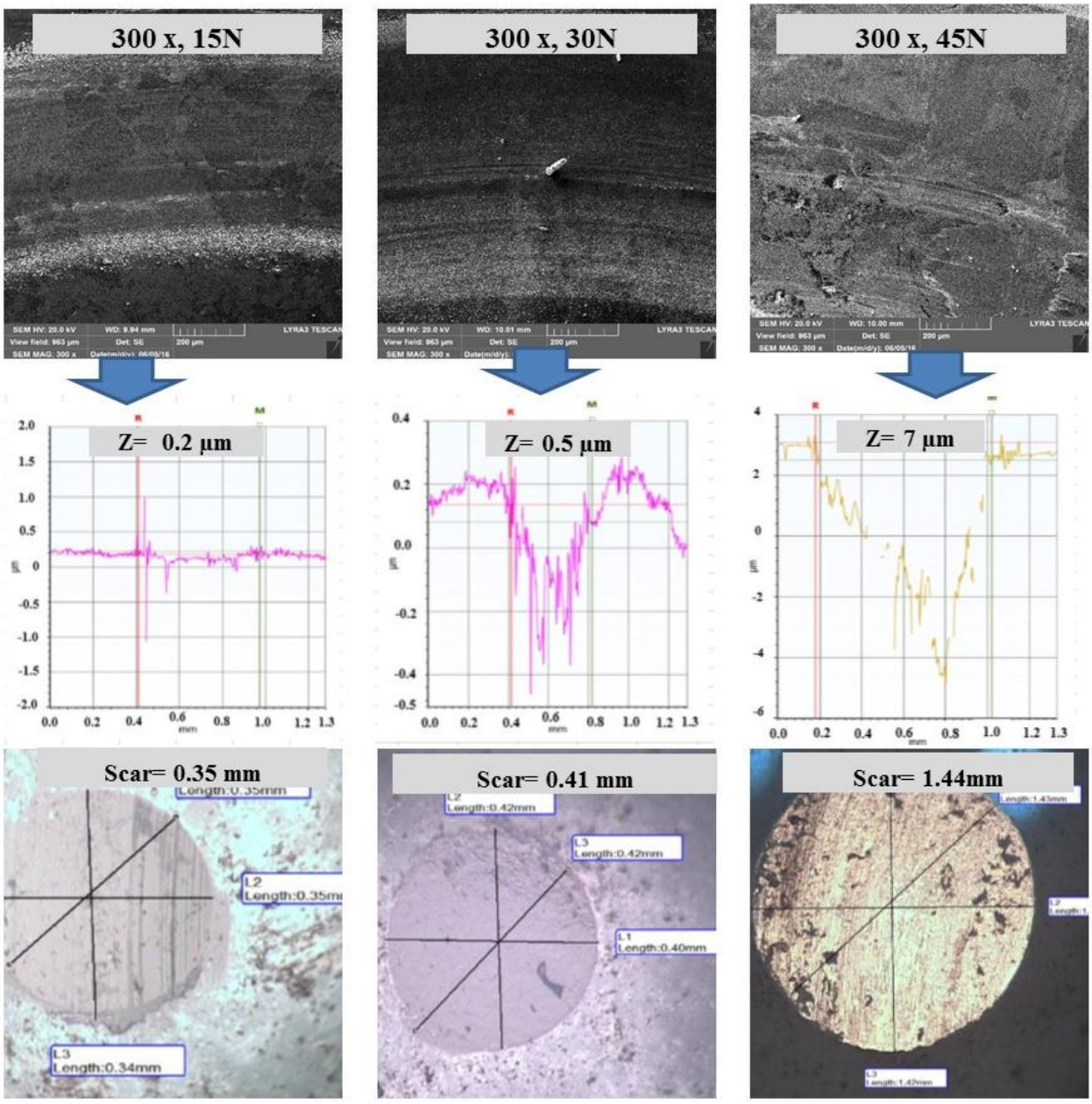

Figure 25: Summary of results of the nano size tests at different loads, each SEM image is related to a 2-D profile and and scar mark of counterface ball.

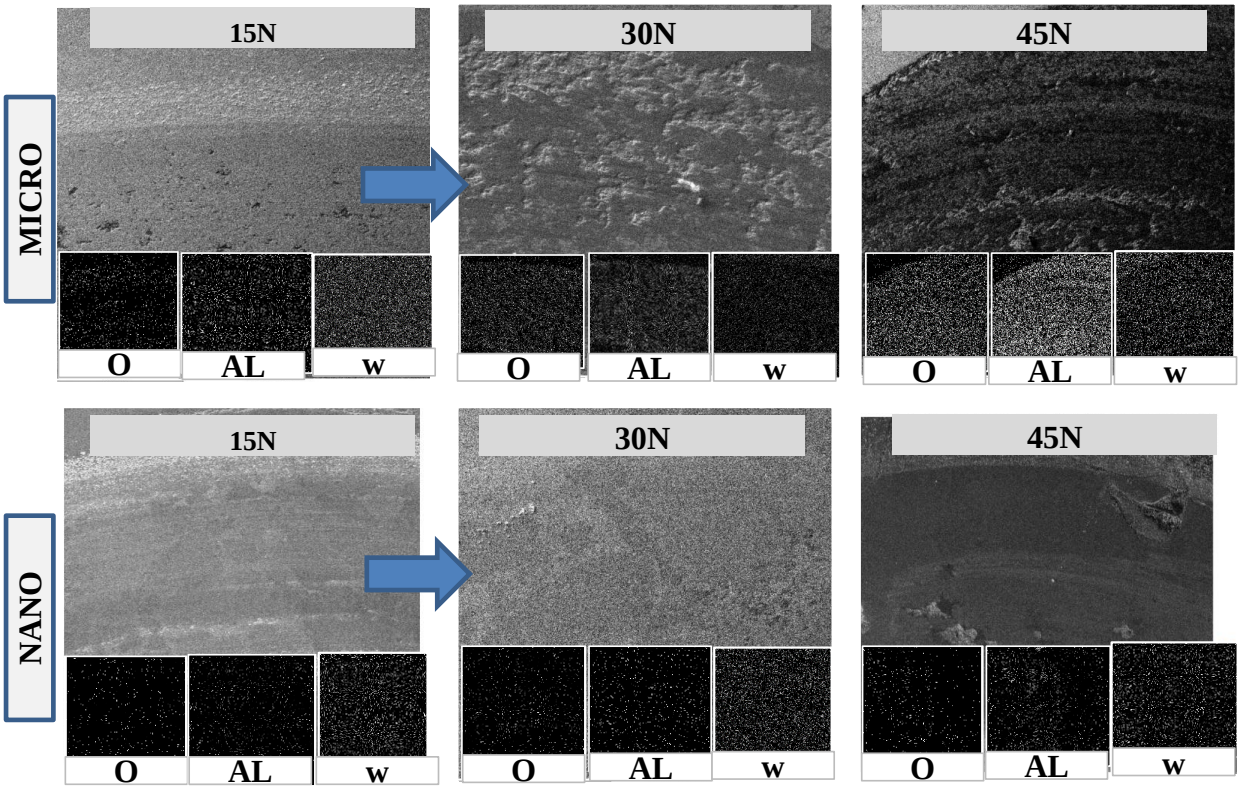

Figure 26: EDS Mapping for the wear track of a micro/nano samples after the wear test conducted at different normal loads and a constant sliding speed of 0.1 m/s.

4.2.2 Effect of speed on coefficient of friction and wear rate

Variation in specific wear rates with varying speeds (0.1, 0.2 and 0.4 m/s) for both the micron and nano sized WC samples at a constant normal load of 30 N are shown in Figure 27. Figure 28 shows the variation of COF with changing linear speed. Wear rate was observed to increase with increasing speed for both sizes of WC. This can be attributed to the rise in localized temperature which could be very high at higher speeds, leading to a sharp increase in the wear rate due to the changes in the thermal properties of the interface materials [12]. Moreover, with an increase in the sliding speed, the time available for the heat dissipation decreases and hence the rise in the localized temperature gets magnified which in turn makes the interface material soft and easy to be pulled-out. This can be observed in the specific wear rate values obtained at higher speeds for

both the micron sized and nano sized samples whereby the soft binder (cobalt) softens at higher localized temperatures resulting in the deboning of the WC particles resulting in higher wear rates. However, it is to be noted that the specific wear rates for the nano sized WC samples was lower than the micron sized WC samples at all speeds and this again can be attributed to the improved bonding between the soft binder with the WC particles due to an increase in the effective surface area. The same trend of increased wear profile depths and the size of the scar mark on the counterface alumina ball with increasing speeds can be observed from Figure 28. All runs showed a steady state condition throughout the test time and all tests showed the same behavior for the friction. Figure 29 shows typical graphs of coefficient of friction at the same sliding speed for the nano sized WC and for the micro sized WC and Figure 30 shows a typical wear track of one run of 3 mm radius at normal load of 30N and at sliding speed of 0.1m/s.

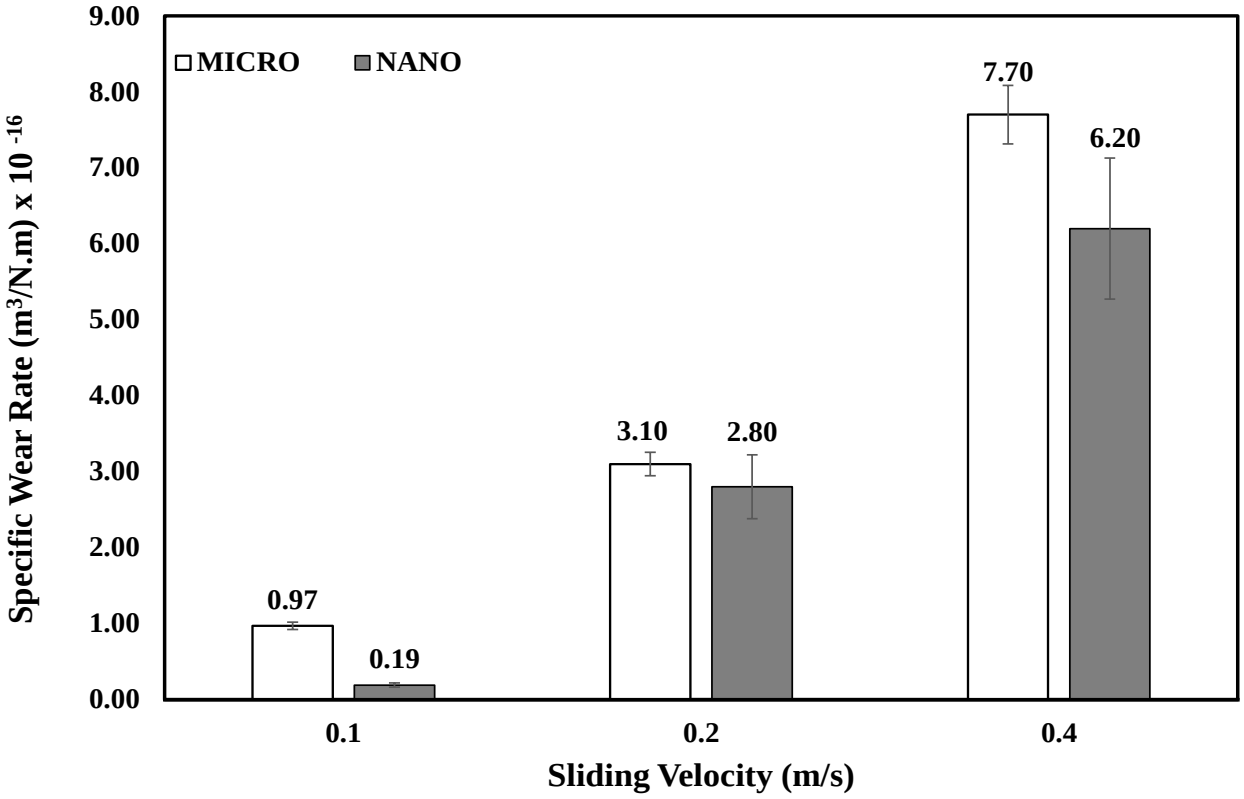

Figure 27: Variation of specific wear rate with different sliding speeds at a constant normal load of 30N

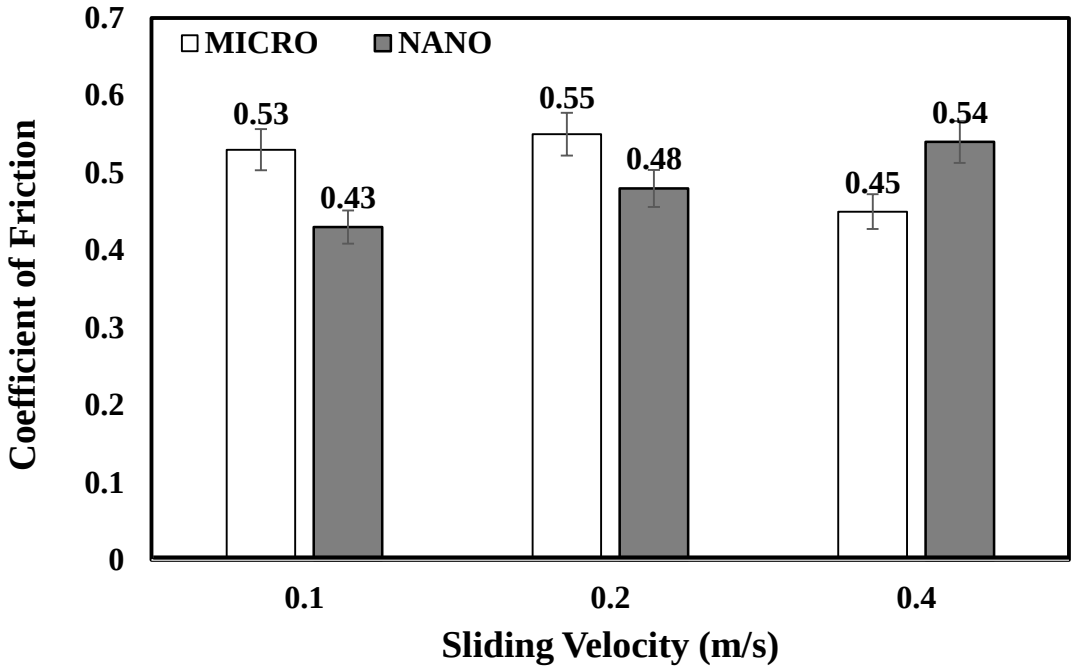

Figure 28: Coefficient of friction of micro and nano WC at different sliding velocity and at a constant normal load of 30N

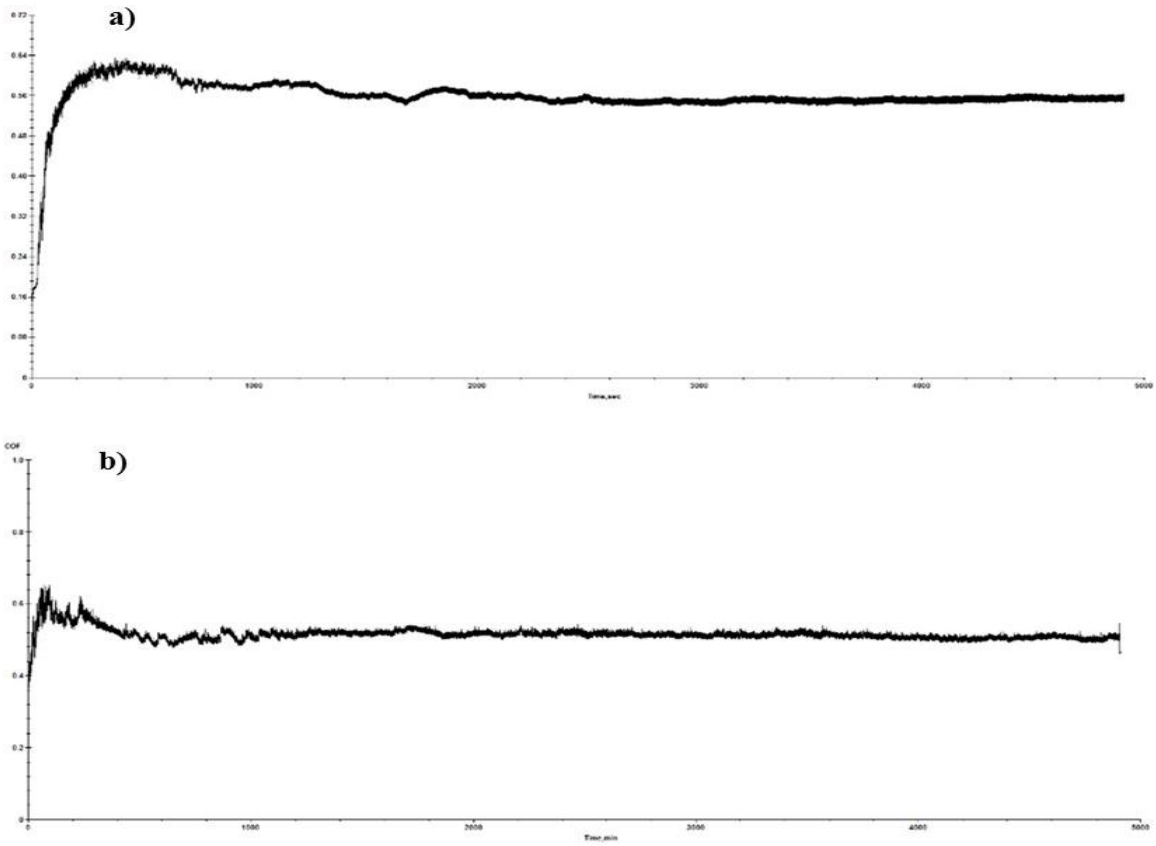

Figure 29: Typical graphs of coefficient of friction at same sliding speed, a) Nano sized WC at normal load of 45N and sliding speed of 0.1m/s with mean coefficient of friction of 0.56, b) Micro sized WC at normal load of 30N and sliding speed of 0.1m/s with mean coefficient of friction of 0.53

Figure 30: Typical wear track of 3 mm radius at normal load of 30N and at sliding speed of 0.1m/s

Figure 31 and Figure 32 summarize the wear track characteristics for micron size and nano size respectively at different speeds of 0.1, 0.2 and 0.4 m/s at a constant load of 30 N and after a sliding

distance of 500 m. Wear tracks were analyzed using SEM imaging at 300x magnification, followed by 2-D optical profiling of each wear track and optical images of alumina counterface ball. SEM images of the wear tracks of micron size show the debris of alumina counterface trapped inside the wear track area as confirmed from the EDS analysis of the wear tracks (*Figure 33*). It can be observed that the depth of the wear track increased as the speed increases, signifying an increase in the wear rate. Figure 32 shows the wear track characteristics of the nano sized WC samples. The SEM images and the profiles show that the wear track area and depth is larger at higher speeds. The size of the scar mark on the counterface ball as seen from the optical images (Figure 32 and Figure 32) after the wear tests done at different speeds for both micro and nano sizes show an increasing trend with increasing speeds. But it is to be noted that the scar mark on the ball in the case of the ball sliding against the nano sized WC samples is lower than the ball sliding against the micron sized WC samples confirming the lower wear rate observed in case of the nano sized samples. This again can be attributed to the improvement in the bonding between the softer and the harder phases due to an effective increase in the surface area. The EDS mapping conducted on the wear tracks after the tests for both the micron and nano sized WC samples confirms the presence of wear debris particle on the wear track as shown in *Figure 33*. However, the amount of wear debris in case of the nano sized samples was much less when compared to that of the micron sized samples, suggesting the improvement in the wear resistance of the nano sized samples at room temperature. Figure 34 shows EDS spectra of the wear track area for both particle sizes at sliding speed of 0.1 m/s and normal load of 45N and found that the amount of alumina debris is higher in the micron sized WC.

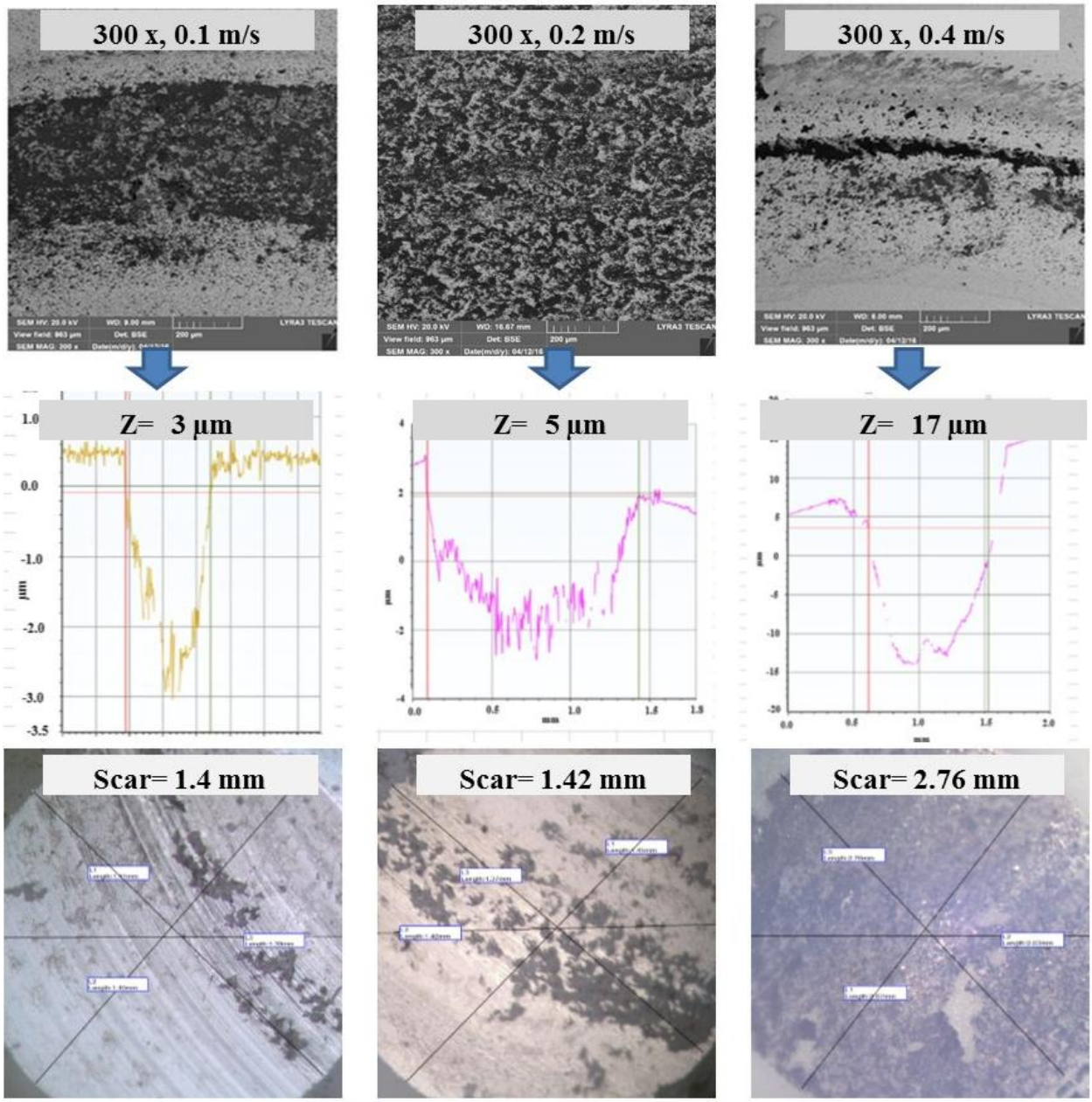

Figure 31: Summary of results of the micron size tests at different speeds, each SEM image is related to a 2-D profile and and scar mark of counterface ball.

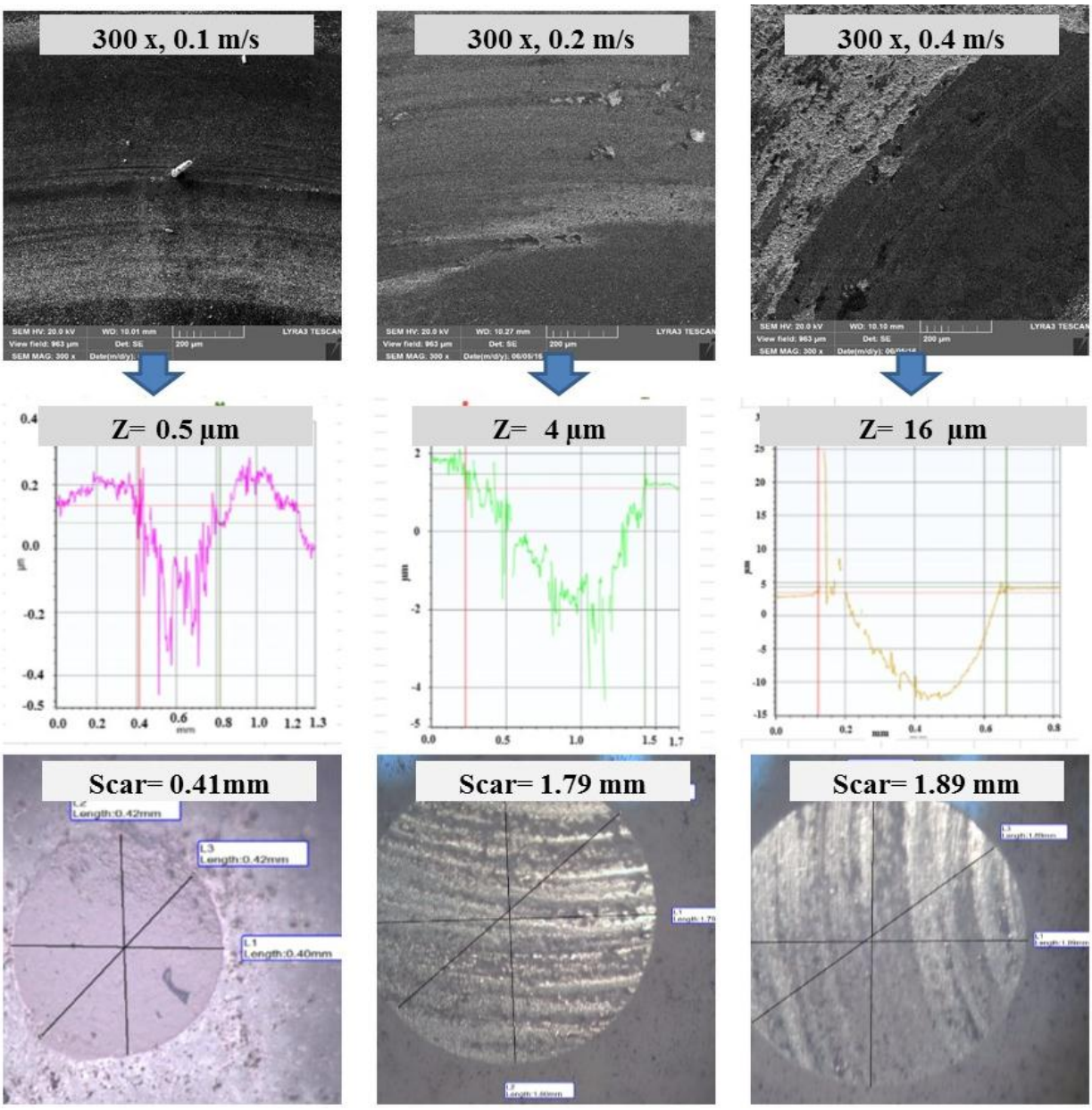

Figure 32: Summary of results of the nano size tests at different speeds, each SEM image is related to a 2-D profile and scar mark of counterface ball.

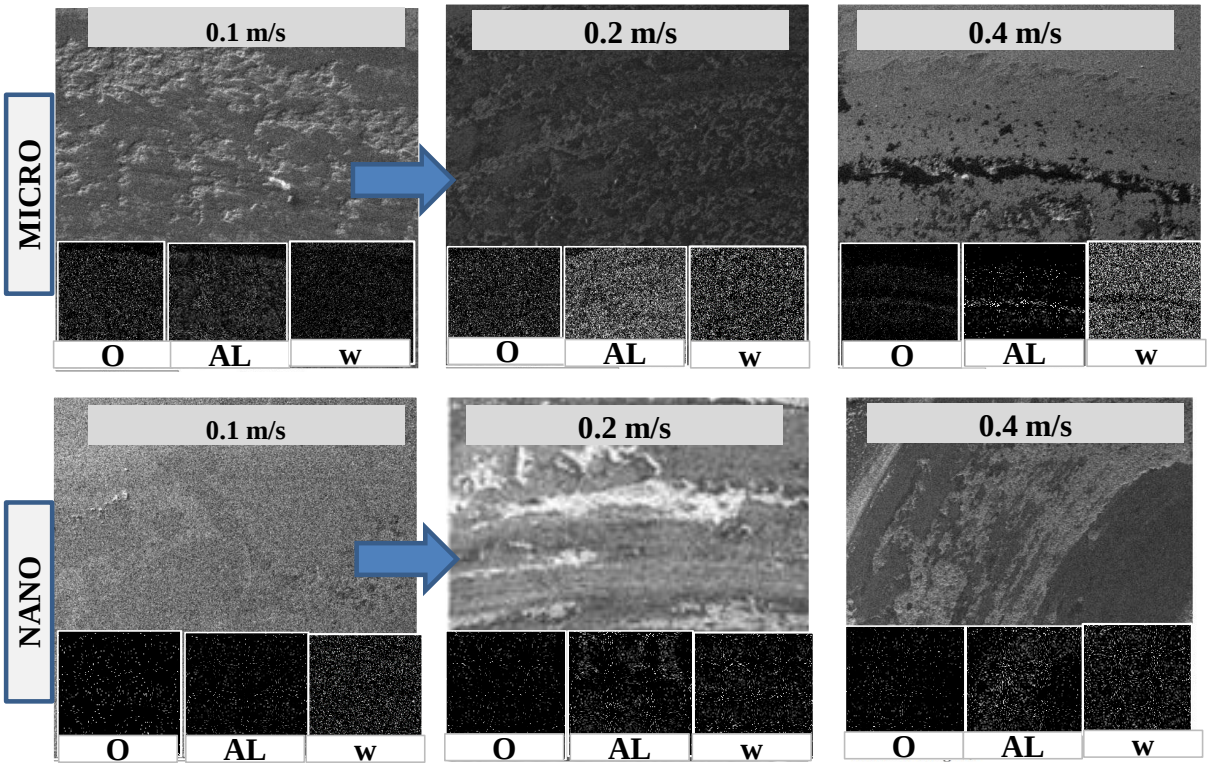

Figure 33: EDS Mapping for the wear track area of a micro/nano samples after the wear test conducted at different linear speeds and a constant normal load of 30N.

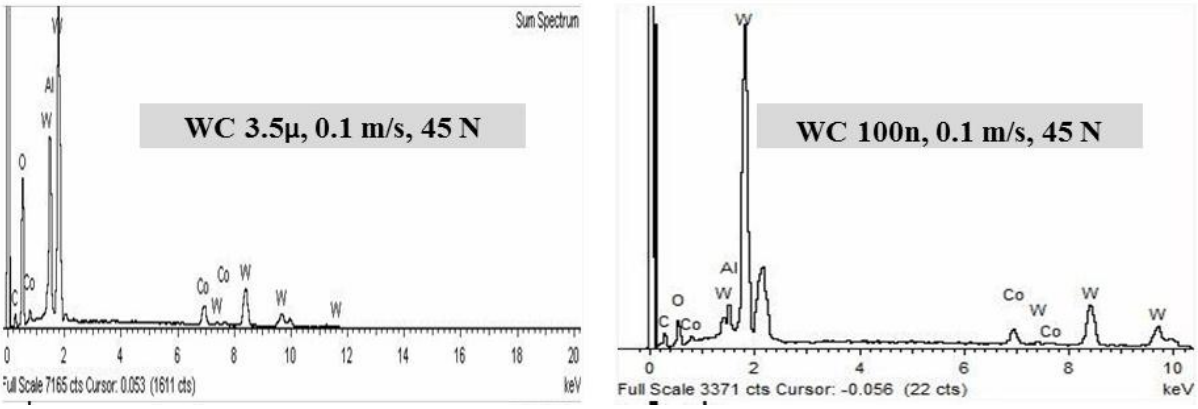

Figure 34: EDS spectra of the wear track area at sliding speed of 0.1 m/s and normal load of 45N inside the wear track area for the micron sized and the nano sized WC.

4.3 PHASE III: Tribological characterization at Elevated Temperatures

4.3.1 Effect of temperature on coefficient of friction and wear rate

Average wear rates at different temperatures (Room Temperature - 300˚C- 600˚C) for both the micron and nano sized WC samples are shown in Figure 35, for a normal load of 30 N and a linear speed of 0.1 m/s. As can be observed from the figure, the specific wear rate shows an increasing trend for both the sizes of WC samples with an increase in temperature. However, it is interesting to note that at higher temperatures (300 and 600^0C), the nano sized WC samples show higher wear rate than the micron sized WC samples. At a temperature of 600^0C, the specific wear rate of the nano sized WC samples increased by 99.6 % as compared to that at room temperature. This deterioration in the wear resistance of the nano sized WC samples at elevated temperatures is attributed to the higher oxidation of the nano sized WC particles due to an increase in their surface area which is also confirmed by the TGA and XRD characterization as presented later.

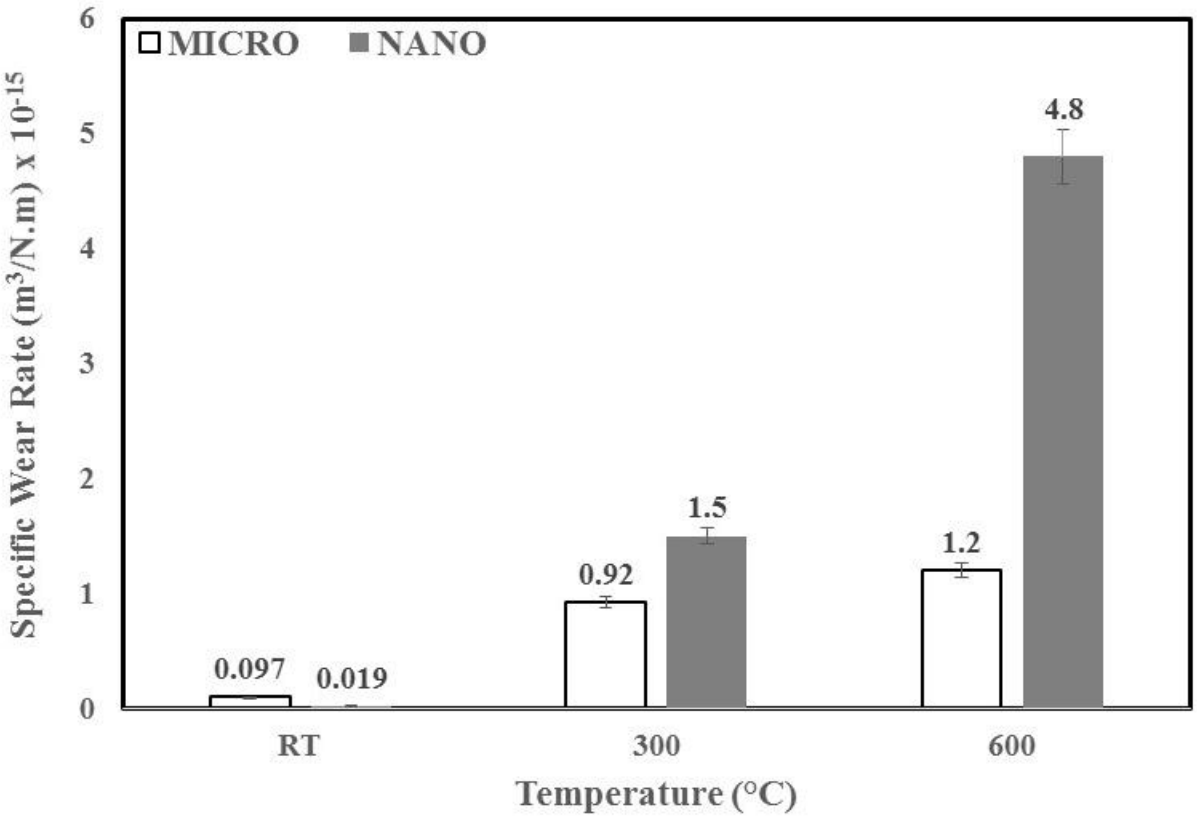

Figure 35: Variation of specific wear rate with different temperatures at sliding velocity of 0.1m/s and at a constant normal load of 30N

The friction of cemented carbides at different temperature are shown in Table 7. In comparison of friction between each particle size, at all temperature at different sizes of WC the friction is in the same range of 0.43-1.15.

Table 7: Coefficient of friction at different temperatures for both particle size of WC at sliding velocity of 0.1m/s and at a constant normal load of 30N

	RT	300 °C	600 °C
MICRO	**0.53 ±0.03**	**0.5 ±0.02**	**1.15 ±0.02**
NANO	**0.43 ±0.07**	**0.64 ±0.04**	**0.52 ±0.03**

All experiments showed a steady state condition throughout the test time and all tests showed the same behavior for the friction and Figure 36 shows this test of micron size with a mean coefficient of 0.51. The test was carried out at speed of 0.1m/s and at load of 30N. This indicates that the parameters chosen were sited properly the samples were dense and homogenous.

Also, all experiments gave steady forces during testing and Figure 37 shows Fx and Fz during testing of nano sized WC at temperature of 300˚C. There was a small variation in the temperature during testing, but this variation was too small and can be neglected. Figure 38 shows variation of test temperature of nano sample at 300˚C, that small variation is not affecting the friction and the temperature sensor of the furnace was designed to keep the furnace at the same temperature. All tests were fixed at the same fixed temperature and all of variations can be assumed to be so close to the desired testing temperature and this variation is acceptable.

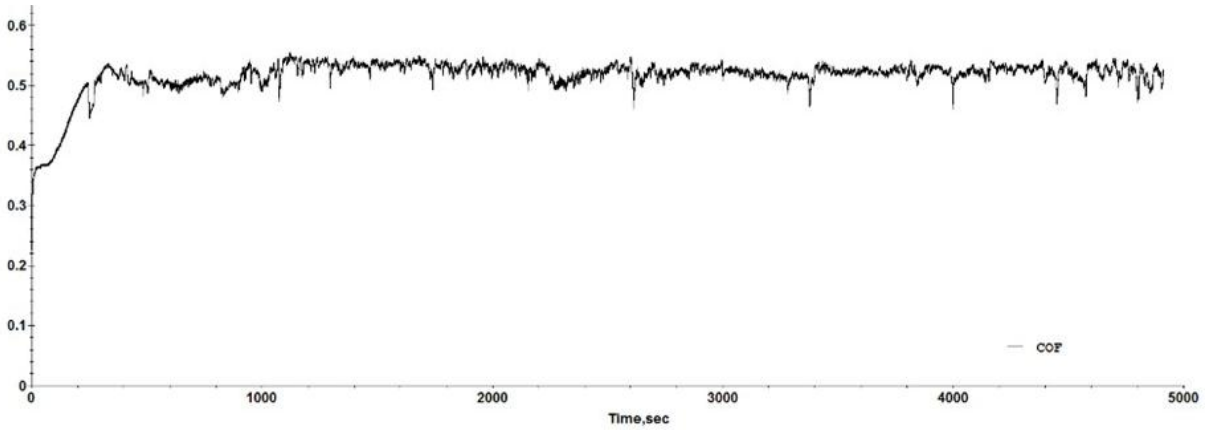

Figure 36: Coefficient of friction with time for micron size WC at temperature of 300°C with a mean of 0.51

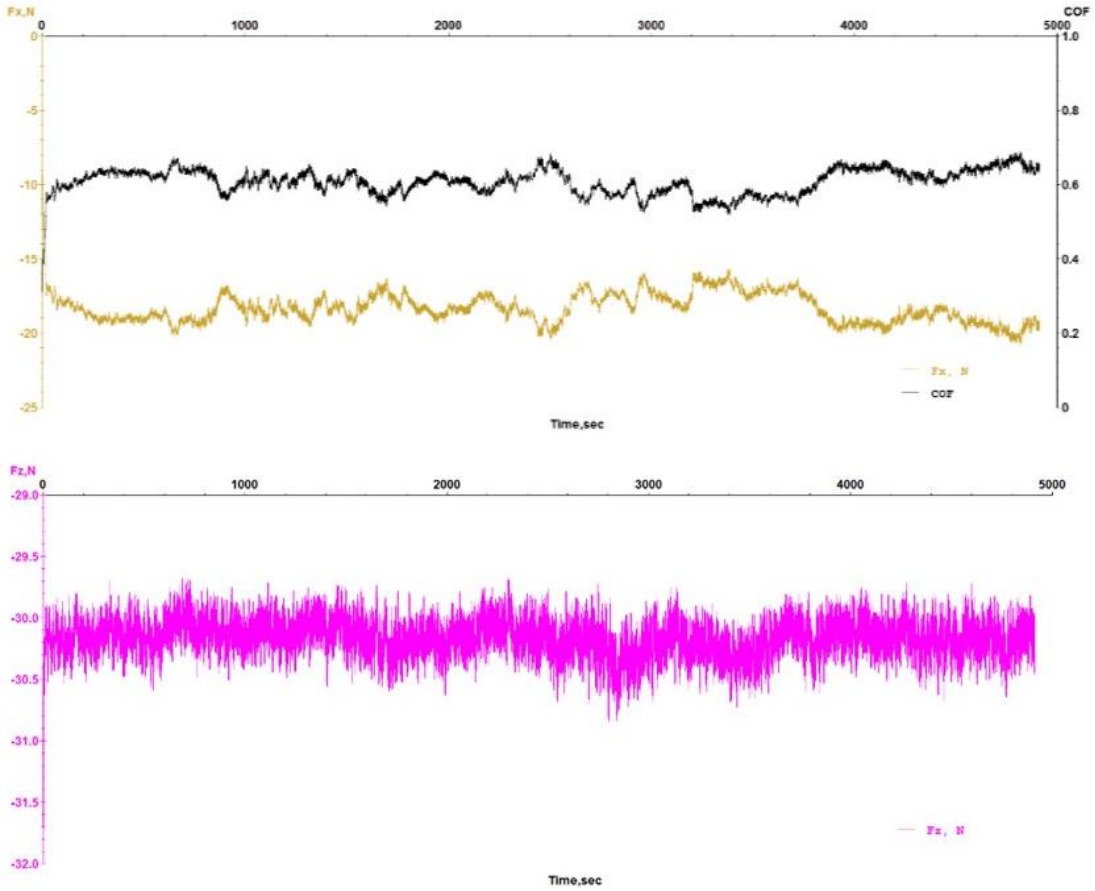

Figure 37: Coefficient of friction and forces (F_X,F_Z) during test of nano sample of WC at temperature of 300°C with mean of 0.64

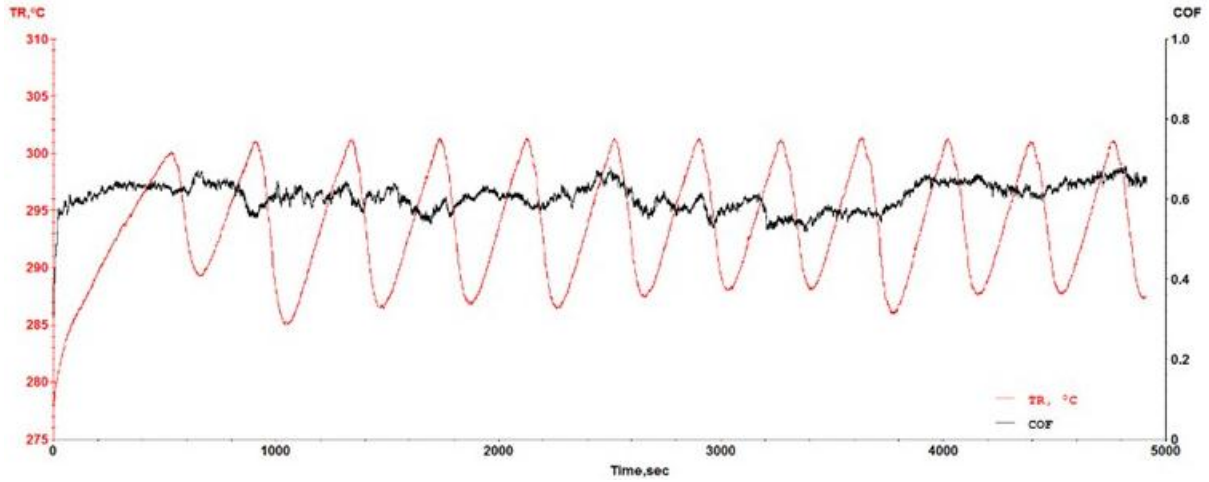

Figure 38: Coefficient of friction of nano WC at 300°C and variation of temperature with time during testing with mean of 0.64

Figure 39 and Figure 40 show the wear track characteristics for micron sized and nano sized WC samples respectively at different temperatures of RT, 300˚C and 600˚C. Wear tracks were analyzed using SEM imaging at 300x magnification, followed by 2-D profiling using an optical profilometer and recording the scar mark on the counterface ball using an optical microscope. In Figure 39 and Figure 40 both SEM images and profile's images confirm that as temperature increased the wear rate showed an increasing trend at a linear speed of 0.1 m/s and normal load of 30N for both the micron and the nano sized WC samples by showing deeper wear tracks at 300˚C and 600˚C. The increased wear rate in both the samples is attributed to the increased oxidation of the WC particles at elevated temperatures leading to a reduction in the wear resistance of the material. However, the nano sized WC samples showed higher wear rates than the nano sized WC samples at elevated temperatures of 300 and 600^0C. This is mainly attributed to the higher oxidation rate of the nano sized WC samples due to their increased surface area as compared to that of the micron sized WC samples, thus confirming the oxidative wear as the predominant wear mechanism at higher temperatures. The formation of oxides at higher temperatures has a detrimental effect on the mechanical properties of WC-9%Co leading to poor wear performance [48].

However, at room temperature, the performance of the nano sized WC samples showed much better performance than the micron sized WC samples, both in case of the wear track depths and the scar mark diameters. This better performance is attributed to the increased surface area in case of the nano sized WC samples leading to an increase in the effective area available for efficient bonding between the hard WC particles and the soft Co binder and hence making the material pull-out much difficult leading to higher wear resistance.

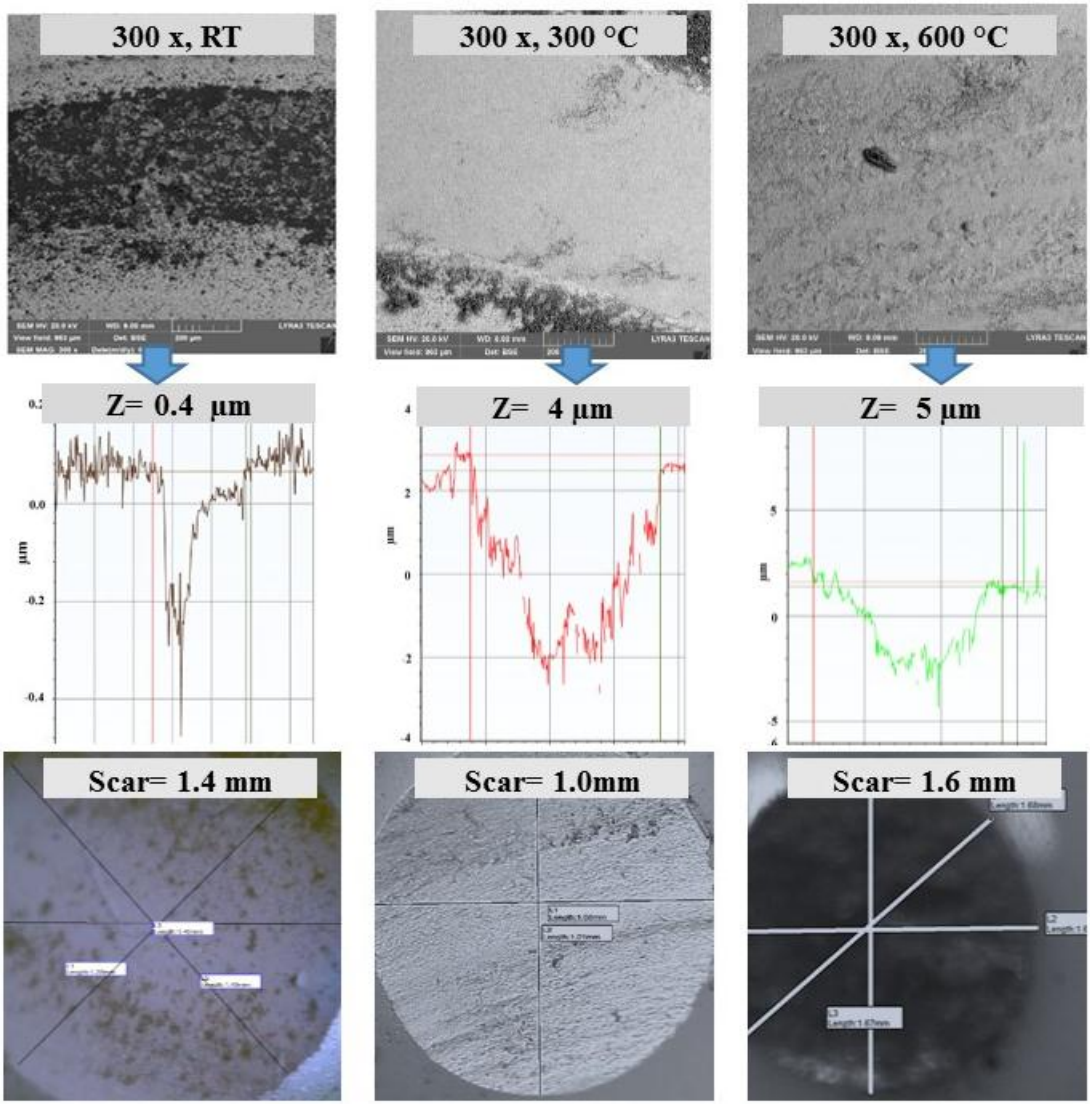

Figure 39: SEM images, 2D profile images of the wear tracks and the corresponding counterface ball images after the wear tests conducted at a load of 30N, at a speed of 0.1 m/s and at different temperatures of RT, 300 and 6000C respectively for the micron sized WC samples.

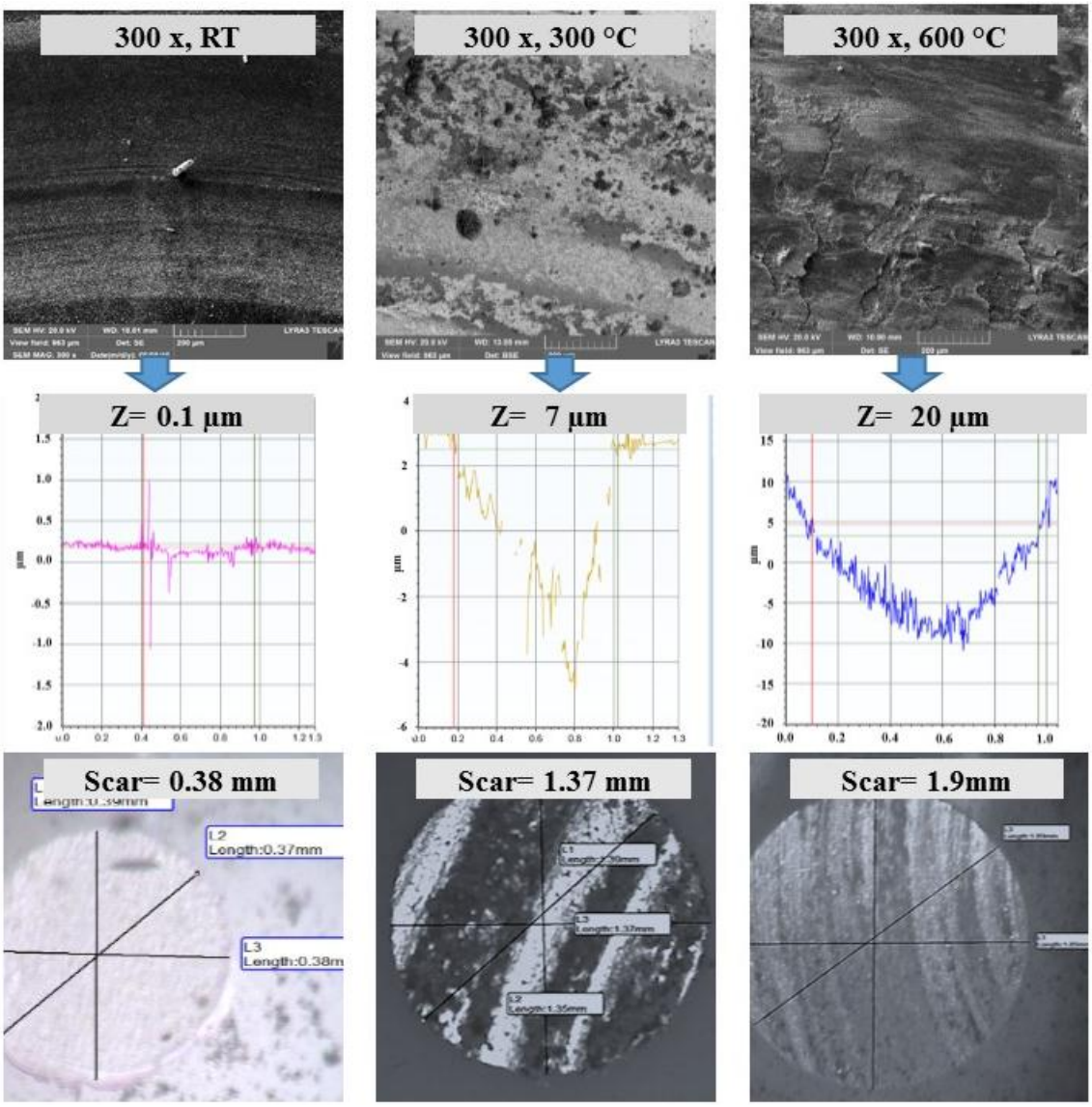

Figure 40: SEM images, 2D profile images of the wear tracks and the corresponding counterface ball images after the wear tests conducted at a load of 30N, at a speed of 0.1 m/s and at different temperatures of RT, 300 and 6000C respectively for the nano sized WC samples.

Optical images of alumina counterface after the wear tests were carried out at different temperatures for both micro and nano sizes. The samples were first cleaned with acetone and three readings of diameters of scar marks were taken. Figure 39 and Figure 40 also show the optical images of the alumina counterface ball after the wear tests at different temperatures for both micro

and nano sized WC samples. Cemented carbide debris was found to be transferred on the alumina counterface as observed from the optical images. As can be seen from scar diameters of the counterface ball images, the size of the scars increased with temperature when slid against both the micron sized and nano sized WC samples signifying an increase in the wear rate with temperature in both the cases. However, it is to be noted that the scar mark diameter on the balls slid against the nano sized WC samples was higher than the balls slid against the micron sized WC samples at higher temperatures of 300 and 600^0C, signifying an increase in wear for the nano sized WC samples at elevated temperatures.

4.3.2 Wear Track Area Characterization

To further understand the underlying wear mechanisms and to evaluate the reasons for the higher wear rates of the nano sized WC samples as compared to that of the micron sized WC samples, EDS analysis was conducted on the wear tracks for both the sets of samples. Figure 41 shows SEM/EDS spectrums conducted on the wear tracks formed at temperatures of 300 °C and 600 °C on both the micron and nano sized WC samples after the wear test. Interestingly, the formation of oxides on the surface can be clearly seen on the wear tracks for all the samples after the wear tests at elevated temperatures as is indicated by an increase in the intensity of the oxygen peak as with increasing temperature. It is to be noted that the weight percent of oxygen on the wear track increased from 14.12 to 25.93 for the micron sized WC samples and from 21.59 to 31.52 for the nano sized WC samples as the temperature increased from 300 to 600^0C suggesting an increase in the oxidation rate with temperature. Moreover, it is to be noted that the oxygen content at 300 and 600^0C is higher for the nano sized WC samples (21.59 wt.%, 31.52 wt.%) as compared to that of the micron sized WC samples (14.12 wt.%, 25.93 wt.%) respectively, suggesting an increase in the oxidation rate for the nano sized WC samples at higher temperatures. Figure 42 shows SEM

images for the wear track of nano samples at room temperature and at 600 °C, the tungsten oxide (WO_3) is apparent to cover the wear track for the sample at 600 °C. Figure 43 shows a nano sized WC sample inside the heating chamber of the UMT-3 tribometer immediately after the wear test at 600° C. The oxide layers can be clearly seen on the surface of the sample. It has been observed in various earlier studies that at higher temperatures, the WC tends to form a metal-oxide compound that of tungsten oxide (WO_3) [48]. Moreover, the oxide layer thickness was found to be increasing considerably with increasing test temperature and ultra-fine cemented carbides [44]. WO_3 was also found to be the dominant kind of oxide formed by the WC hardmetals at elevated temperature with Co as matrix with other inhibitors like Ni and Cr [49]. So, to further confirm the formation of WO_3, a TGA and XRD analysis was conducted. Figure 44 shows the TGA result of WC heated up to 600 °C in air which clearly shows an increase in weight with increasing temperature until 600 °C suggesting of oxidation and formation of metal-oxide compounds. After the TGA analysis, the WC sample was subjected to a XRD characterization to ascertain the formation of tungsten oxide (WO_3). Figure 45 shows the XRD spectrum conducted on the WC sample immediately after the TGA analysis. It confirms the formation of tungsten oxide (WO_3) after matching with the data base spectrum of WC (ICDD 00-051-0939) and tungsten oxide (ICDD 01-072-0677). The spectrum reveals that most of the WC (~10%) has been transferred into WO_3 (~90%).

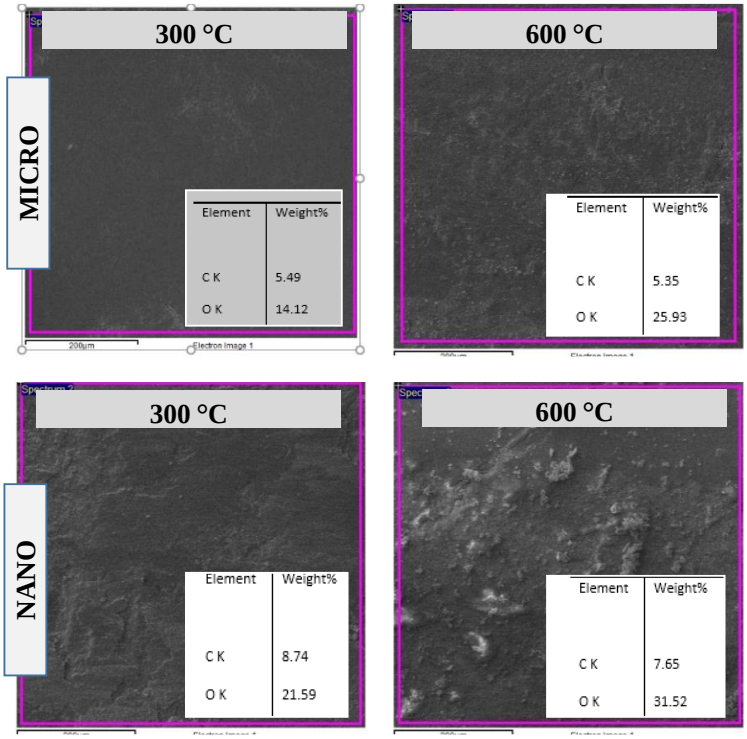

Figure 41: EDS analysis conducted on the wear tracks for the micron sized and the nano sized WC samples after the wear test at a load of 30N, a speed of 0.1 m/s and at temperatures of 300 and 600^0C respectively.

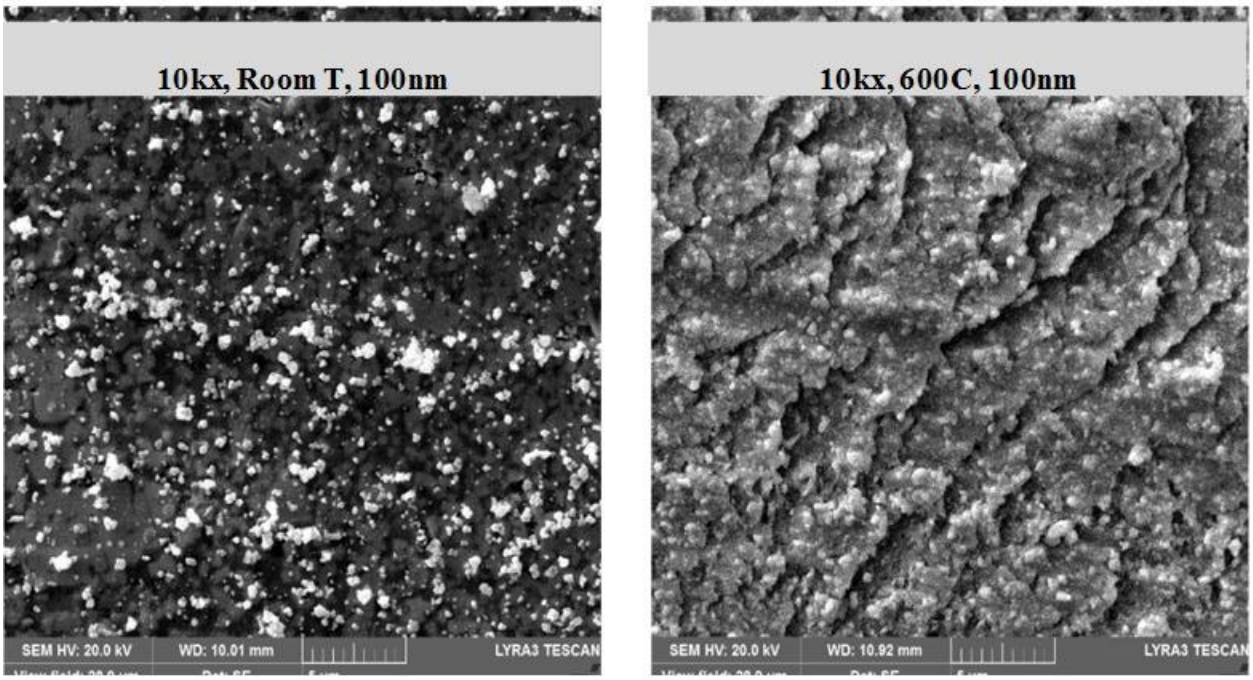

Figure 42: SE SEM images of 10kx magnification of nono size samples at room temperature and at 600 °C.

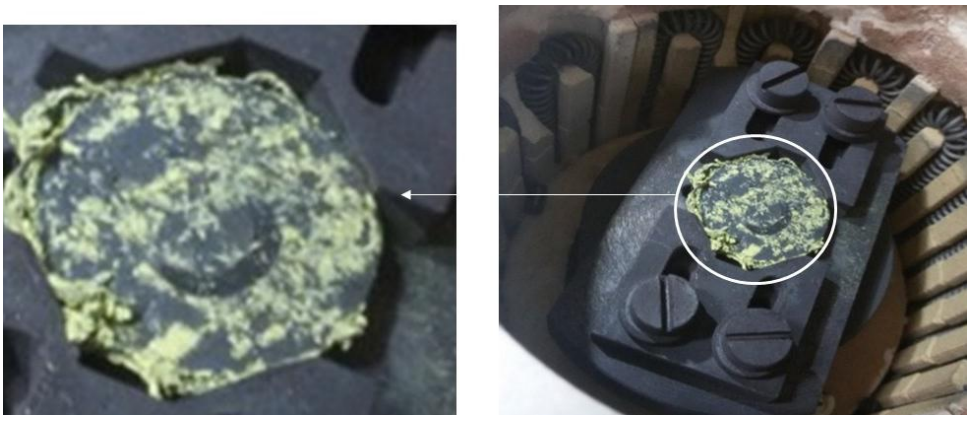

Figure 43: Nano sized WC-9%Co sample after the wear test at a normal load of 30N, speed of 0.1 m/s and at 600°C.

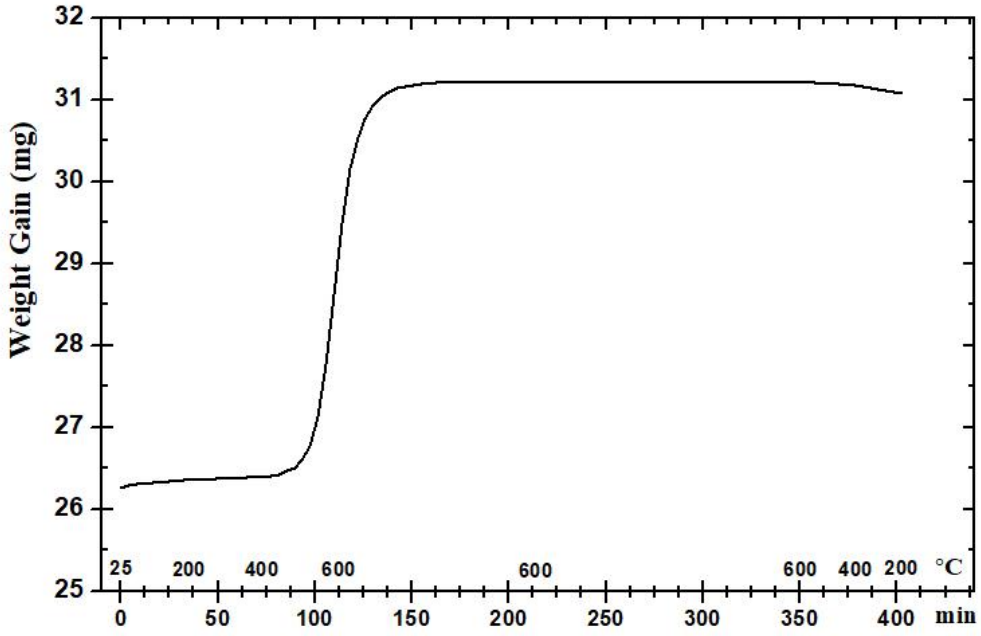

Figure 44: TGA result of WC weight gain versus time until a temperature of 600 °C.

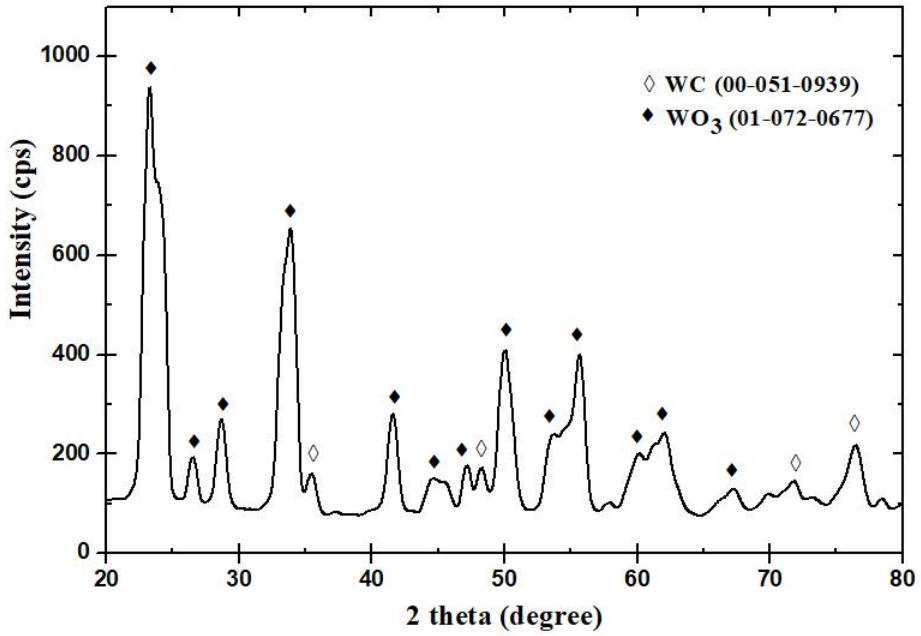

Figure 45: XRD spectrum of the WC sample Intensity measure of resulted compound after the TGA test as compared to the data base spectrum of tungsten oxide (WO_3).

4.3.3 Underlying Wear Mechanisms

As can be seen from the above presented results of the different characterization techniques (EDS, TGA, XRD), the oxidation of WC leading to the formation of the WO_3 is confirmed for both the micron sized and nano sized WC samples at elevated temperatures of 300 and 600^0C respectively. Moreover, the amount of oxides is found to be increasing with temperature for both the samples with greater amount of oxides for the nano sized samples as compared to that of the micron sized samples. This is mainly attributed to the increased available surface area in the nano sized WC samples for oxidation. Hence in view of the above characterization results coupled with the examination of the SEM images of the wear tracks after the tests, it can be concluded that the wear mechanisms for both the micron and the nano sized samples at elevated temperatures is a combination of abrasive and oxidative wear, with the oxidative wear playing a significant role resulting in a greater material loss.

CHAPTER 5

5. CONCLUSIONS

Micron (3.5 µm) and nano sized (100 nm) sized WC powders were used to synthesize samples of WC-9%Co using spark plasma sintering process. The tribological properties were evaluated at different normal loads (15N, 30N and 45N) and different linear speeds (0.1m/s, 0.2m/s and 0.4m/s) under (room temperature, 300°C and 600°C) conditions. Based on the results, the following conclusions can be drawn.

1. The sintering parameters of both micro and nano particle size by the spark plasma sintering (SPS) resulted in dense and hard bulk samples. The observed density and hardness for the 3.5 µm WC were 13.77 (g/cm^3), 93.9% densification and 1411 (Hv_{30}), while the observed density and hardness for the 100 nm WC were 13.62 (g/cm^3), 92.8% densification and 1495 (Hv_{30}).
2. The nano sized WC samples showed improved wear resistance at different normal loads and different linear speeds at room temperature as compared to the micron sized WC samples. This is attributed to the effective increase in the surface area in the nano sized WC samples resulting in improved bonding between the softer binder (cobalt) and the hard WC particles leading to a significant resistance to material pull-out and wear.
3. However, with an increase in temperature the performance in terms of wear resistance of the nano sized samples decreased significantly as compared to the micron sized samples. This is attributed to the increased oxidation of the nano particles due to their higher surface area.
4. It was observed that the abrasive wear accelerated by oxidative wear is the predominant wear mechanism for both sizes of WC at elevated temperature, and showed that wear rate at

temperature of 600°C is lower by 75% for the micron size as compared to the nano size WC-9 wt.% Co.

5.1 FUTURE WORK

- ✓ Applying the tests at different temperature conditions.
- ✓ Investigating the tribological aspects at lubricated conditions.
- ✓ Evaluation of wear at different Co content and with amore additives and inhibitors.
- ✓ Evaluation of wear at lower particle size of nano cemented carbides.
- ✓ Comparing the same results at different sintering techniques.

REFERENCES

[1] T. Laoui, O. Blest, "Effect of TiC addition on the microstructure and properties of Ti(C,N)-WC-Co-Ni cermet," *journal of materials science letters,* vol. 13, pp. 1530-1532, 1994.

[2] N. Al-Aqeeli, N. Saheb, T. Laoui, "The synthesis of nanostructured WC-based hardmetals using mechanical alloying and their direct consolidation," *journal of nanomaterials,* 2014.

[3] H. Ortner, P. Ettmayer, H. Kolaska, "The history of the technological progress of hardmetals," *international journal of refractory metals and hard materials,* vol. 44, p. 148–159 , 2014.

[4] T. Sailer, M. Herr, H. Sockel, "Microstructure and mechanical properties of ultrafine-grained hardmetals," *international journal of refractory metalt and hard materials,* vol. 19, pp. 553-559, 2001.

[5] H. Juhr, H. Schulze, G. Wollenberg, "Improved cemented carbide properties after wire-EDM by pulse shaping," *journal of materials processing technology,* pp. 553-559, 2004.

[6] H. Engqvist, G. Botton, S. Ederyd, "Wear phenomena on WC–based face seal rings," international journal of refractory metals and hard materials, vol. 18, pp. 39-46, 2000.

[7] L. Llanes, Y. Torres, M. Anglada, "On the fatigue crack growth behavior of WC–Co cemented carbides: kinetics description, microstructural effects and fatigue sensetivity," acta materialia, vol. 50, pp. 2381-2393, 2002.

[8] B.Casas, Y. Torres, L. Llanes, "Fracture and fatigue behavior of electrical discharge machined cemented carbides", international journal of refractory metals & hard materials, vol. 24, pp. 162-167, 2006.

[9] M. Gee, A. Gant, B. Roebuck, "Wear mechanisms in abrasion and erosion of WC/Co," *wear,* vol. 263, pp. 137-142, 2007.

[10] G. Shao, X. Duan, J. Xie, "Sintring of nanocrystalline WC–Co composite powder," advanced material science, vol. 5, pp. 281-286, 2003.

[11] B. Mortimer, J. Lancaster, "Extending the life of aerospace dry bearings by the use of hard smooth counterfaces," wear, vol. 121, pp. 289-305, 1988.

[12] R. Merwe, N. Sacks, "Effect of TaC and TiC on the friction and dry sliding wear of WC–6 wt.% Co cemented carbides against steel counterfaces," *international journal of refractory metals and hard materials,* vol. 41, p. 94–102, 2013.

[13] S. Hewitt, T. Laoui, K. Kibble, "Effect of milling temperature on the synthesis and consolidation of nanocomposite WC–10Co powders," *international journal of refractory metals & hard materials,* vol. 27, p. 66–73, 2009.

[14] N. Novikov, V. Bondarenko, V. Golovchan, "High temperature mechanical properties of WC–Co hard metals," *journal of super hard materials,* vol. 29, no. 5, p. 261–280, 2007.

[15] S. Hewitt, T. Laoui, "Synthesis of nanocomposite WC-Co powders by high-energy ball milling," 2007.

[16] A. Lisovskii, "On the development of nanostructured WC–Co hard alloys," *journal of super hard materials,* vol. 32, no. 6, p. 389–395, 2010.

[17] C. Allen, M. Sheen, J. Williams, "The wear of ultrafine WC–Co hard metals," *wear,* vol. 250, p. 604–610, 2001.

[18] Z. Fang, X. Wang, T. Ryu, K. Hwang, "Synthesis, sintering and mechanical properties of nanocrystalline cemented tungsten carbide – a review," *international journal of refractory metals & hard materials,* vol. 27, p. 288–299, 2009.

[19] Y. Milman, "The effect of structural state and temperature on mechanical properties and deformation mechanisms of WC–Co hard alloy," *journal of superhard materials,* vol. 36, no. 2, p. 65–81, 2014.

[20] S. Ndlovu, K. Durst, M. Goken, "Investigation of the sliding contact properties of WC-Co hard metals using nanoscratch testing," *wear,* vol. 263, p. 1602–1609, 2007.

[21] P. Krakhmalev, T. Rodil, J. Bergstrom, "Influence of microstructure on the abrasive edge wear of WC–Co hardmetals," *wear,* vol. 263, p. 240–245, 2007.

[22] S. Okamoto, Y. Nakazono, K. Otsuka, "Mechanical properties of WC/Co cemented carbide with larger WC grain size," *material characterization,* vol. 55, p. 281– 287, 2005.

[23] V. Rajinikanth, K.Venkateswarlu, "An investigation of sliding wear behaviour of WC–Co coating," *tribology international,* vol. 44, p. 1711–1719, 2011.

[24] S. Ndlovo, "The wear properties of tungsten carbide-cobalt hardmetals from the nanoscale up to the macroscopic scale," 2009.

[25] Q. Zhang, Y. He, W. Wang, N. Lin, "Corrosion behavior of WC–Co hardmetals in the oil-in-water emulsions," *corrosion science,* vol. 94, p. 48–60, 2015.

[26] Y. Delgado, P. Baets, K. Bonny, "Influence of wire-EDM on high temperature sliding wear behavior of WC-10Co(Cr/V) cemented carbide," *int. journal of refractory metals and hard materials,* vol. 41, p. 198–209, 2013.

[27] H. Saito, A. Iwabuchi, T. Shimizu, "Effects of Co content and WC grain size on wear of WC cemented carbide," *wear,* vol. 261, p. 126–132, 2006.

[28] K. Bonny, P. Baets, J. Vleugels, "Impact of Cr3C2/VC addition on the dry sliding friction and wear response of WC–Co cemented carbides," *wear,* vol. 267, p. 1642–1652, 2009.

[29] J. Pirso, M. Viljus, S. Letunovit, "Friction and dry sliding wear behaviour of cermets," *wear,* vol. 260, p. 815–824, 2006.

[30] G. Quercia, I. Grigorescu, H. Contreras, "Friction and wear behaviour of several hard materials," *international journal of refractory metals,* vol. 19, pp. 359-369, 2001.

[31] L. Espinosa, A. Borrell, M. Salvador, "Sliding wear behavior of WC–Co–Cr3C2–VC composites fabricated by conventional and non-conventional techniques," *wear,* vol. 307, p. 60–67, 2013.

[32] N. Al-Aqeeli, K. Mohammad, T. Laoui, N. Saheb, "VC andCr3C2 doped WC-based nano-cermets prepared by MA and SPS," *ceramics international,* vol. 40, p. 11759–11765, 2014.

[33] L. Espinosa, V. Bonache, M. Salvador, "Friction and wear behaviour of WC–Co–Cr3C2–VC cemented carbides obtained from nanocrystalline mixtures," *wear,* vol. 272, pp. 61-68, 2011.

[34] K. Bonnya, P. Baets, Y. Perez, J. Vleugels, "Friction and wear characteristics of WC–Co cemented carbides in dry reciprocating sliding contact," *wear,* vol. 268, p. 1504–1517, 2010.

[35] B, Casas, M. Cardellach, J. Alcalá, "Influencia de la temperatura sobre la resistencia al desgaste de pares idénticos de WC–Co," *VIII congreso nacional de propiedades mecánicas de sólidos,* 2002.

[36] J. Zunega, M. Gee, R. Wood, J.Walker, "Scratch testing of WC/Co hardmetals," *tribology international,* vol. 54, p. 77–86, 2012.

[37] Y. Delgado, K. Bonny, P. Baets, P. Neis, "Dry sliding friction and wear response of WC-Co hardmetals pairs in linearly reciprocating and rotating contact," *sustainable construction and design,* 2011.

[38] K. Bonny, P. Baets, B. Lawers, J. Vleugels, "Charactrization of tribological behaviour of hardmetals," Ghent University, Belgium.

[39] J. Pirso, S. Letunovits, M. Viljus, "Friction and wear behaviour of cemented carbides," *wear,* vol. 257, p. 257–265, 2004.

[40] T. Kagnaya, C. Boher, L. Lambert, M. Lazard, "Wear mechanisms of WC–Co cutting tools from high-speed tribological tests," *wear,* vol. 267, p. 890–897, 2009.

[41] D. Jianxin, Z. Hui, W. Ze, L. Yunsong, "Friction and wear behaviors of WC/Co cemented carbide tool materials with different WC grain sizes at temperatures up to 600 °C," *international journal of refractory metals and hard materials,* vol. 31, p. 196–204, 2012.

[42] H. Chen, G. Gou, M. Tu, "Research on the friction and wear behavior at elevated temperature of plasma-sprayed nanostructured WC-Co coatings," *ASM intrnational,* vol. 19, pp. 1-6, 2010.

[43] Q. Yang, T. Senda, A. Hirose, "Sliding wear behavior of WC–12% Co coatings at elevated temperatures," *surface & coatings technology,* vol. 200, p. 4208– 4212, 2006.

[44] X. Shi, H. Yang, G. Shao, X. Duan, "Oxidation of ultrafine-cemented carbide prepared from nanocrystalline WC–10Co composite powder," *ceramics international,* vol. 34, p. 2043–2049, 2008.

[45] E. Marui, H. Endo, A. Ohira, "Wear test of cemented tungsten carbide at high atmospheric temperature 400C," *tribology letters,* vol. 8, pp. 139-145, 2000.

[46] H. Zhang, J. Deng, G. Li, X. Ai, "Effect of ambient temperature on wear of cemented carbide tool material," *advanced materials research,* Vols. 148-149, pp. 276-279, 2011.

[47] T. Laoui, A. Hakeem, K. Abdullahi, "Spark plasma sintering of mixed and milled WC-Co micro-/nanopowders," *advanced materials research,* Vols. 284-286, pp. 537-543, 2011.

[48] Wesmann, J. N. Espallargas, "Effect of atmosphere, temperature and carbide size on the sliding friction of self-mated HVOF WC–CoCr contacts," *tribology international,* vol. 101, p. 301–313, 2016.

[49] L M. Aristizabal, L. Ardila, F. Veiga, M. Arizmendi, "Comparison of the friction and wear behaviour of WC–Ni–Co–Cr and WC–Co hardmetals in contact with steel at high temperatures," *wear,* Vols. 280-281, p. 15– 21, 2012.

VITAE

Saleh Abdullah Al Wohaibi

Engineer Officer at the Royal Air Force of Saudi Arabia

Mechanical Engineering Department

King Fahd University for Petroleum and Minerals

Dhahran – Eastern Province – Saudi Arabia

Email: salehwoh@gmail.com

Education BS: Mechanical Engineering, KFUPM (2012)

MS: Mechanical Engineering, KFUPM (2017)

Research Interests Aircraft Maintenance and its Management, Supply Chain Management, Risk Management, Quality Managements, Hard Materials, Tribology, Nanotechnology, Cutting Tools Applications, Corrosion, Material Structure and Defects, Material Characterization Techniques, Spark Plasma Sintering, Welding Applications and Metallurgy, Fatigue and Fracture.

Papers

1. **Wohaibi Saleh,** M. Abdul Samad, Taher Laoui, Faheemuddin Patel, Abbas Hakeem. "**Tribological properties of hardmetals at room and elevated temperatures: A Review"** (Ready for Submission)
2. **Wohaibi Saleh,** M. Abdul Samad, Taher Laoui, Faheemuddin Patel, Abbas Hakeem. "**Tribological Characterization of Micro/Nano WC - 9%Co Cemented Carbide prepared by Spark Plasma Sintering Technique"** (Submitted)
3. **Wohaibi Saleh,** M. Abdul Samad, Taher Laoui, Faheemuddin Patel, Abbas Hakeem, Akeem Yousof. "**Tribological Characterization of Micro/Nano WC - 9%Co Cemented Carbide prepared by Spark Plasma Sintering Technique at Elevated Temperatures"** (Ready for Submission)